2019 Association of Biomolecular Resource Facilities Multi-Laboratory Data-Independent Acquisition Study

Authors

Benjamin A. Neely[1], Paul M. Stemmer[2], Brian C. Searle[3], Laura E. Herring[4], LeRoy Martin[5], Mukul K. Midha[3], Brett S. Phinney[6], Baozhen Shan[7], Magnus Palmblad[8], Yan Wang[9], Pratik D. Jagtap[10], Joanna Kirkpatrick[11,12*]

Affiliations

1. Chemical Sciences Division, National Institute of Standards and Technology, Charleston, SC, USA
2. Wayne State University, Detroit, MI, USA
3. Institute for Systems Biology, Seattle, WA, USA
4. UNC Proteomics Core Facility, Department of Pharmacology, University of North Carolina at Chapel Hill, Chapel Hill, NC, USA
5. Waters Corp., Beverly, MA, USA
6. University of California Davis, Davis, CA, USA
7. Bioinformatics Solutions Inc., Waterloo, ON, Canada
8. Center for Proteomics and Metabolomics, Leiden University Medical Center, Postzone S3-P, Postbus 9600, 2300 RC Leiden, The Netherlands
9. National Institute of Dental and Craniofacial Research, National Institutes of Health, Bethesda, MD, USA
10. Department of Biochemistry, Molecular Biology and Biophysics, University of Minnesota, Minneapolis, MN
11. Leibniz Institute on Aging (FLI), Beutenbergstr 11, 07745, Jena Germany
12. The Francis Crick Institute, 1 Midland Road, London NW1 1AT, UK

*corresponding author(s): Joanna Kirkpatrick (joanna.kirkpatrick@crick.ac.uk)

Abstract

Despite the advantages of fewer missing values by collecting fragment ion data on all analytes in the sample, as well as the potential for deeper coverage, the adoption of data-independent acquisition (DIA) in core facility settings has been slow. The Association of Biomolecular Resource Facilities conducted a large interlaboratory study to evaluate DIA performance in laboratories with various instrumentation. Participants were supplied with generic methods and a uniform set of test samples. The resulting 49 DIA datasets act as benchmarks and have utility in education and tool development. The sample set consisted of a tryptic HeLa digest spiked with high or low levels of four exogenous proteins. Data are available in MassIVE MSV000086479. Additionally, we demonstrate how the data can be analysed by focusing on two datasets using different library approaches and show the utility of select summary statistics. These data can be used by DIA newcomers, software developers, or DIA experts evaluating performance with different platforms, acquisition settings and skill levels.

Background & Summary

Data-independent acquisition (DIA) is an alternative strategy to data-dependent acquisition (DDA) of MS2 fragmentation data in mass spectrometry. In DDA the instrument selects and fragments MS1 ions based on signal intensity. In DIA the mass spectrometer fragments analytes in predefined *m/z* windows. The MS2 data contribute to analyte identification and provide relative quantification. Both DDA and DIA approaches rely on sophisticated algorithms, and the interpretation of data is computationally intensive [1-4]. Benefits of DIA include increased depth of coverage and between-sample uniformity (by to avoiding the stochastic nature of DDA acquisition), allowing unprecedented depth[5] and speed[6] of analysis. Recently, advances in instrumentation and algorithms have resulted in wider adoption[7-9]. In keeping with the mission of the Association of Biomolecular Resource Facilities (ABRF), the Proteomics Research Group (PRG) developed a multi-laboratory study (Figure 1), providing novice and expert users with samples and generic methods to benchmark their laboratories and empower participants to perform DIA.

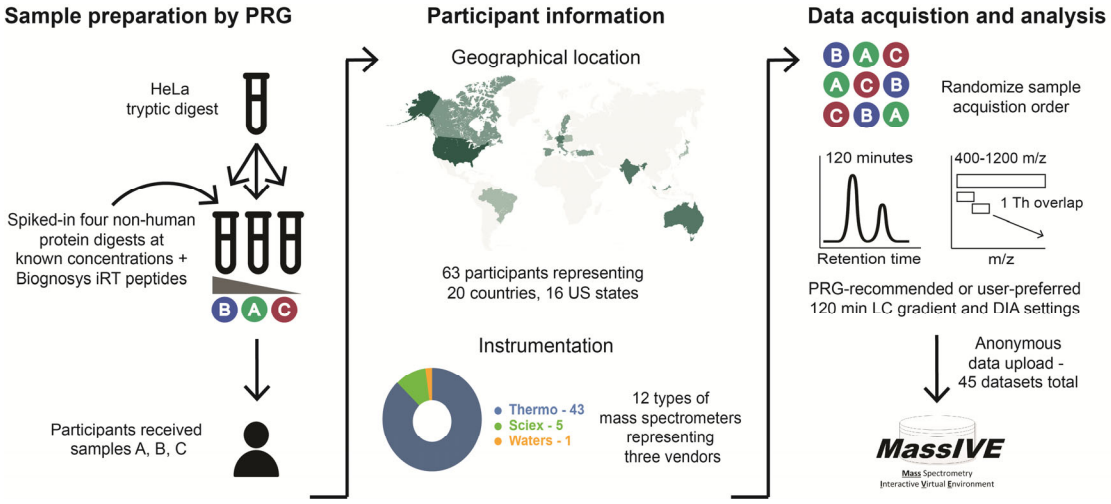

Figure 1. General description of study. The base sample in the study was a tryptic HeLa digest. Each participant received 20 ug of that sample as well as 20 ug of that sample with 2.5 or 10 fmol/µg of four non-human proteins: beta-galactosidase, lysozyme C, glucoamylase, and protein G. All samples also contained an internal retention time (iRT) peptide mix. Participants received dried samples identified only as A, B, or C. Participant identification was confidential and they could identify their dataset through a randomized identification number. Recommended LC and DIA settings were distributed with the samples though participants could use their preferred settings. Each lab was asked to run the samples in a specific randomized manner. Participants anonymously uploaded data to MassIVE, where it was curated by the PRG (renamed if needed and checked for file integrity) and re-uploaded to MassIVE MSV000086479.

Mixtures of proteomes[10,11] have been used to benchmark proteomic workflows. We selected a set of four non-endogenous proteins in a human matrix[12]. The proteins: beta-galactosidase, lysozyme C, glucoamylase, and protein G were digested then spiked into the HeLa digest at 0, 2.5 and 10 fmol/µg (sample A - 2.5 fmol spike; sample B - 10 fmol spike, sample C was no spike). The four added proteins and two levels provided a wide range in signal intensities of the peptides, such that depth of spike-in coverage could reflect relative sensitivity between participants[13,14]. The study announcement was disseminated on the PRG website[15], at conferences and via social media. Participants had varying prior experience and included mass spectrometers from different vendors (Figure 2; Table 1). A generic method (Supplemental File 1) was supplied and participants were asked to use a standard two-hour, two-step LC-gradient, a uniform static overlapping windowing strategy and a cycle time of approximately 3.5 s. Most participants followed these recommendations, (Table 2; Online-only Table 1). Of 63 laboratories that enrolled and received sample sets, 45 returned data. Some users had

multiple instruments or compared different DIA methods, resulting in 49 datasets, 43 of which contain data for all replicates.

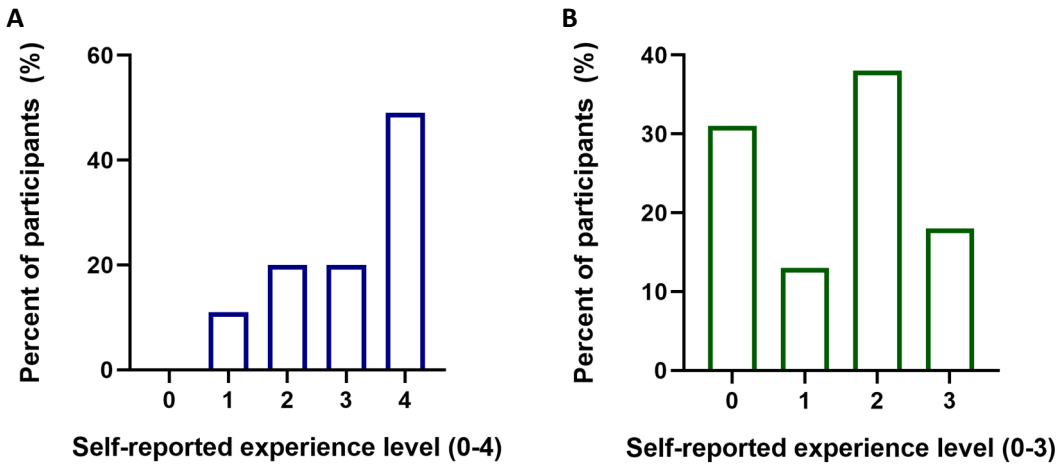

Figure 2. Self-reported experience level of 45 participants. An arbitrary scale was given to participants in a companion survey. **A. Self-reported experience LC-MS/MS level.** When asked about LC-MS/MS experience, participants were given the following choices: 0, "never set up myself"; 1, 0 to 2 years; 2, 3 to 5 years; 3, 6 to 9 years; 4, >10 years. **B. Self-reported DIA experience.** When asked about DIA experience participants were given the following choices: 0, Heard about it; 1, Tried it once; 2, Have done it a couple of times; 3, Expert.

Table 1. Instruments used in the study. The 45 participants deposited 49 datasets using 12 different instrument platforms from three different manufacturers.

Instruments	# datasets
Thermo LTQ Orbitrap Elite	1
Thermo LTQ Orbitrap Velos	1
Thermo Orbitrap Fusion	9
Thermo Orbitrap Fusion Lumos	12
Thermo Orbitrap Velos Pro	1
Thermo Q Exactive	3
Thermo Q Exactive HF	6
Thermo Q Exactive HF-X	7
Thermo Q Exactive Plus	3
Sciex TripleTOF 5600	3
Sciex TripleTOF 6600	2
Waters Xevo G2 XS	1

Table 2. Window scheme strategies used in the study. The DIA window strategies were divided into groups based on whether the DIA windows were static (i.e., the size did not change) and whether the DIA windows overlapped, while five datasets had gaps between the DIA windows.

window scheme	# datasets
variable	2
static, non-overlap	3
static, w/overlap	37
static, w/gaps	5
single window	1
other*	1

** used a targeted list*

Table 3. Flow rates used in the study. There were two main flow rates employed, either nL/min flow rates (approximately 300 nL/min; 250 to 400 nL/min), or µL/min flow rates (1.5 to 50 µL/min).

flowrate	# datasets
~300 nl/min	38
> 1 µL/min	6
unknown	5

Online-only Table 1. Meta information on 49 datasets. This table is available in MassIVE MSV000086479, but shown here for reference.

participant	reported LC-MS/MS experience (0-4)	reported DIA experience (0-3)	method version	complete data set?	acqisition time	flow rate	gradient summary	Instrument	MS1 range	MS1 Res	MS1 max IT	MS2 Res	MS2 max IT	MS2 window range	number MS2 windows	DIA window width	cycle time	DIA window type
1	2	3		yes	0-145	300 nL/min	PRG	Q Exactive HF-X	150-2000	120000	200	15000	22	386-1016	70	9	2.94	static, non-overlap
3	3	2		yes	10-145	300 nL/min	PRG	Orbitrap Fusion	393-1200	120000	20	15000	30	393-1200	62	14	3.97	static, 1 Th overlap
4	3	1		yes	0-165	250 nL/min	supplemental	LTQ Orbitrap V	none	n/a	n/a	n/a	n/a	n/a	n/a	n/a	n/a	targeted list, not DIA
5	4	2		yes	5-145	400 nL/min		Orbitrap Fusion	399-1200	120000	20	30000	60	399.55-1400.5	40	variable		3.35	variable, some with inconsistent overlap
6	4	0		yes	8-159	missing	PRG	Orbitrap Fusion	399-1200	120000	20	30000	60	399-1200	40	21	3.41	static, 1 Th overlap
7	2	0	15k	yes	0-125	250 nL/min		Orbitrap Fusion	393-1200	120000	50	15000	30	393-1200	62	14	3.46	static, 1 Th overlap
7	2	0	30k	no	0-125	250 nL/min		Orbitrap Fusion	399-1200	120000	50	30000	60	399-1200	40	21	3.54	static, 1 Th overlap
8	2	0		yes	0-140	300 nL/min	PRG	Orbitrap Fusion	399-1200	120000	20	30000	60	399.4547-1218	39	21	3.64	static, 0.0105 Th gap between windows
10	2	0		yes	0-150	300 nL/min	PRG	Q Exactive HF	400-1200	120000	20	30000	60	399-1200	40	21	4.14	static, 1 Th overlap
13	3	2		yes	5-145	300 nL/min	PRG	Orbitrap Fusion	399-1200	120000	20	30000	60	399-1200	40	21	3.74	static, 1 Th overlap
14	4	3		yes	0-100	5 uL/min	supplemental	TripleTOF 6600	350-1250	High resolu	150	High resc	25	393-1200	120	variable	3.33	variable, 1 Th overlap
15	1	0		no	0-145	300 nL/min	supplemental	LTQ Orbitrap El	393-1200	120000	20	15000	100	393-1200	62	14	0.41	static, 1 Th overlap
16	4	3		yes	0-117	5 uL/min	PRG	TripleTOF 6600	ND	>= 30,000	ND	>= 20,00	ND	399.5-1200.5	80	11	3.59	static, 1 Th overlap
17	4	2		yes	0-145	300 nL/min	PRG	Q Exactive HF-X	400-1200	120000	20	30000	60	399-1200	40	21	3.57	static, 1 Th overlap
18	3	3		yes	0-130	300 nL/min	supplemental	Orbitrap Fusion	399-1203	120000	20	30000	60	399-1200	40	21	3.62	static, 1 Th overlap
19	4	0		no	0-135	50 uL/min	supplemental	Q Exactive HF-X	397-1203	120000	20	30000	60	397-1203	23	36	2.26	static, 1 Th overlap
20	3	2		yes	0-120	300 nL/min	supplemental	TripleTOF 5600	400-1200	>= 30,000	250	>= 20,00	40	400-1200	80	11	3.67	static, 1 Th overlap
21	2	2		yes	0-130	300 nL/min	supplemental	Orbitrap Fusion	393-1200	120000	ND	15000	30	393-1200	62	14	3.96	static, 1 Th overlap
23	4	3		yes	xevos	8 uL/min	PRG	Xevo G2-XS Q-	50-2000	30000	n/a	30000	n/a	400-1200	200	25	3.22	scanning, 21 Th overlap, stepping every 4 Th
25	4	0		no	0-150	300 nL/min	PRG	Orbitrap Fusion	393-1200	120000	20	15000	30	393-1200	62	14	3.61	static, 1 Th overlap
26	4	3		yes	0-130	250 nL/min	supplemental	TripleTOF 5600	200-1600	35000 (High	250	15000 (hi	40	400-1200	73	12	3.38	static, 1 Th overlap
28	4	0		yes	0-140	300 nL/min	PRG	Q Exactive HF	399-1200	120000	20	30000	60	399-1200	1	801	0.44	single window
29	4	1		yes	10-120	350 nL/min		Orbitrap Fusion	393-1200	120000	20	15000	30	393-1200	62	14	3.32	static, 1 Th overlap
31	1	2		yes	0-170	300 nL/min	PRG	Orbitrap Fusion	393-1200	120000	20	15000	30	393-1200	62	14	3.97	static, 1 Th overlap
32	4	1		yes	10-120	300 nL/min	supplemental	Orbitrap Fusion	391-1208	120000	20	15000	30	391-1208	48	18	2.67	static, 1 Th overlap
33	3	2		no	25-150	300 nL/min		Orbitrap Fusion	399-1200	120000	20	30000	60	399-1200	40	21	3.5	static, 1 Th overlap
34	3	2		yes	0-145	missing	PRG	Q Exactive HF	399-1200	120000	20	30000	60	399-1200	40	21	3.97	static, 1 Th overlap
35	4	2		yes	0-175	300 nL/min	PRG	Q Exactive HF	400-1200	120000	20	30000	60	399-1200	40	21	4.16	static, 1 Th overlap
36	2	1		yes	0-146	300 nL/min	supplemental	Q Exactive HF	399-1200	120000	20	30000	50	399-1200	40	21	3.67	static, 1 Th overlap
37	1	2		yes	0-130	400 nL/min	PRG	Orbitrap Fusion	399-1200	120000	20	30000	60	399-1200	40	21	3.56	static, 1 Th overlap
39	4	3		yes	0-130	5 uL/min	supplemental	TripleTOF 5600	399-1200	>= 30,000	250	high sen	40	400-1200	80	11	3.66	static, 1 Th overlap
44	4	2		yes	0-140	1.5 uL/min		Q Exactive HF-X	400-1200	120000	20	30000	60	399-1200	40	21	3.54	static, 1 Th overlap
45	4	2		yes	0-150	300 nL/min	PRG	Q Exactive Plus	399-1200	35000	30	17500	60	399.4383-1213	29	30	2.78	static, 1.99 Th overlap
46	4	1	lab	yes	8-142	300 nL/min	supplemental	Orbitrap Fusion	197.08-120	120000	25	30000	54	400.285-1203.(	53	15	4.54	static, 0.15 Th gap between windows
46	4	1	PRG	yes	10-142	300 nL/min	PRG	Orbitrap Fusion	399-1200	120000	20	30000	60	399-1200	40	21	3.49	static, 1 Th overlap
47	2	0		yes	0-150	250 nL/min	supplemental	Q Exactive	400-1000	17500	55	17500	55	400.4373-1000	25	24	2.26	static, 0.011 Th gap between windows
48	4	3	lumos	yes	0-145	300 nL/min	PRG	Orbitrap Fusion	399-1200	120000	20	30000	60	399-1200	40	21	3.38	static, 1 Th overlap
48	4	3	qehfx	yes	0-145	300 nL/min	PRG	Q Exactive HF-X	400-1200	120000	20	30000	60	399-1200	40	21	3.48	static, 1 Th overlap
49	1	2		yes	0-141	missing	PRG	Q Exactive	400-1200	70000	50	17500	55	400.9392-1212	27	31	2.92	static, 0.986 Th overlap
50	4	2		yes	0-145	300 nL/min	supplemental	Q Exactive HF-X	399-1200	120000	20	30000	60	399-1200	40	21	3.34	static, 1 Th overlap
52	4	2		yes	5-150	300 nL/min	PRG	Orbitrap Fusion	400-1000	60000	50	15000	22	350-950	75	8	3.61	static, non-overlap
53	2	0		yes	0-150	missing	PRG	Q Exactive	400-1200	140000	20	35000	60	399-1200	40	21	6.69	static, 1 Th overlap
54	3	0	b	yes	0-140	300 nL/min	supplemental	Q Exactive Plus	350-1200	140000	30	35000	119	349.95-1201.0	45	19.9	9.42	static, 1 Th overlap
54	3	0	h	yes	0-140	300 nL/min	supplemental	Q Exactive Plus	350-1200	35000	55	35000	100	400.4376-1,20	32	25	5.76	static, 0.011 Th gap between windows
55	2	1		no	0-180	300 nL/min	supplemental	Q Exactive HF	400-1200	120000	20	30000	60	399-1200	40	21	4.21	static, 1 Th overlap
56	3	0		yes	0-145	300 nL/min	PRG	Orbitrap Velos	400-1200	30000	ND	7500	ND	400-1200	25	32	5.12	static, non-overlap
57	4	0		yes	0-145	300 nL/min	PRG	Q Exactive HF-X	400-1200	120000	20	30000	60	399-1200	40	21	3.49	static, 1 Th overlap
60	4	0		yes	10-140	missing	supplemental	Orbitrap Fusion	393-1200	120000	20	15000	30	393-1200	62	14	3.4	static, 1 Th overlap
63	1	2		yes	0-150	300 nL/min	supplemental	Orbitrap Fusion	399-1200	120000	20	30000	60	399.4547-1,21	39	21	3.19	static, 0.0105 Th gap between windows

Other studies have used multi-laboratory DIA datasets to benchmark software tools[10,16]. Similarly, this new dataset has many uses, including benchmarking and user training. The range of user experience and instruments contributed to differences in data quality, providing a real-world dataset for evaluating how software normalization strategies are affected by data quality. Incorporation of known spikes facilitates evaluation of relative quantification using DIA [17]. When the spiked proteins are ignored, each participant performed triplicate injections of experimental replicates, allowing for generation of useful summary statistics. Overall, this dataset provides opportunities for users to learn about acquisition methods and evaluate computational tools for DIA.

This dataset is also valuable to DIA software developers. The recommended acquisition method was not optimized for any platform, producing datasets conducted on different platforms with a similar acquisition strategy. All samples included iRT peptides and companion DDA and gas-phase fractionation data were also generated. Therefore, any software or library approach can use the data to evaluate and improve these approaches. The inclusion of the spike proteins in known amounts creates a unique opportunity to test new DIA strategies, such as MS1-based quantification[18] and *in silico* generated libraries[19-23].

In an initial analysis we have made a comparative analysis of data from two participants that used the same instrument. Each acquired additional data for library generation so it was possible to show how library construction and utilization effects results. Library strategy affected the number of proteins identified (Figure 3A-B), the precision of replicates (Figure 3A-B), and relative abundances of spike-in proteins (Figure 3C-D). Similar to reported observations[17] these results highlight discrepancies when inferring protein abundance and the need to check relative quantification across the dynamic range. As these data and associated metadata are publicly available, we expect it to be used in benchmarking new tools and library strategies. Ongoing analysis of the dataset will provide more information and best-practice instrument settings for DIA, though the generic method provided performed unexpectedly well. With continued advancement of DIA methods, platforms optimized for DIA and improved computational strategies, this is an exciting time for the field, and we look forward to future multi-laboratory studies, enabling users and developers alike.

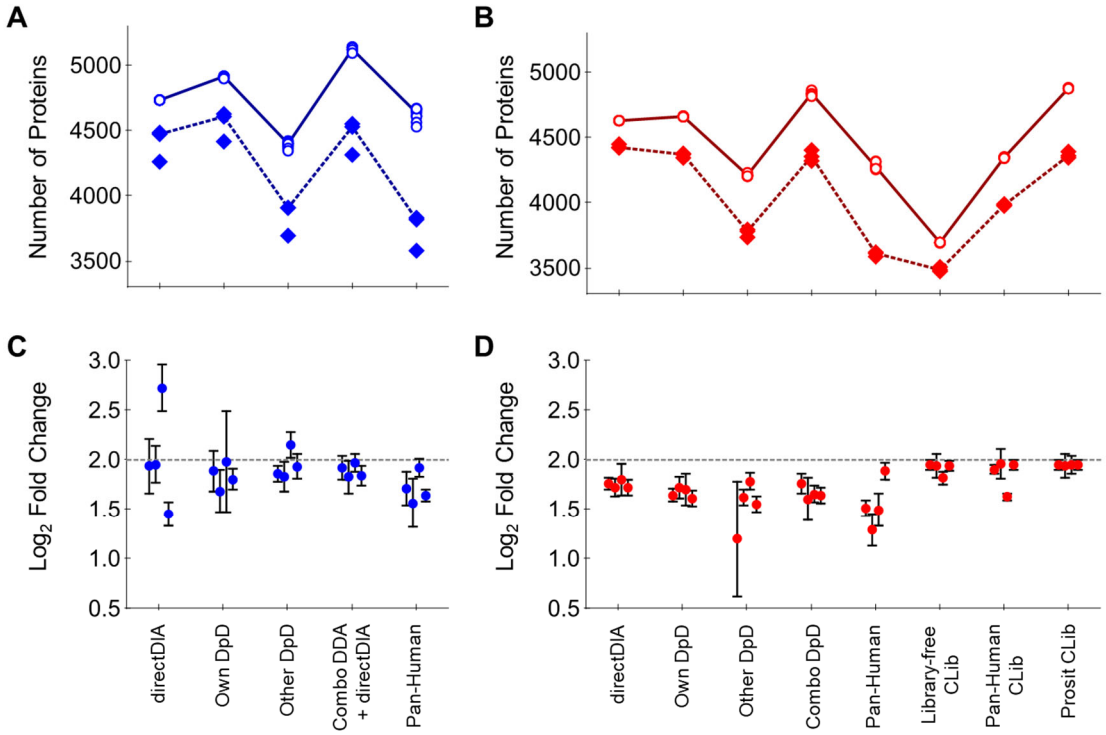

Figure 3. Comparison of library approaches with data from participants 3 and 48. Different library approaches were used to evaluate protein identification, technical variation and accurate relative quantification of four spike proteins with participant 48 **(A and C)** and participant 3 **(B and D)**. Eight library approaches are shown: directDIA, using the DIA files to generate the library; own **DpD** (DDA plus DIA), using the participant's data to generate a library; other DpD, using the other participant's DDA and DIA-based library; combined DpD, a combined library of the DDA and DIA data from both participants; Pan-Human, the Pan-Human library augmented with empirical evidence of the four non-endogenous spike-in proteins; Library-free CLib, chromatogram library; Pan-Human CLib, chromatogram library combined with Pan-human plus spikes; Prosit CLib, chromatogram library with prosit generated spectra. Only participant 3 generated a chromatogram library. **A-B.** Proteins identified using participant 48 data **(A)** or participant 3 data **(B)**. Hollow points are total identifications per sample with solid line being the average identifications. Solid points are number of proteins below 20 % CV with the dotted line being average proteins below 20 % CV. **C-D.** Estimated abundance of the four spike in proteins using the different library approaches for participant 48 **(C)** and 3 **(D)**. Log2 fold-change with 95% confidence intervals for the four spike-in proteins was determined between the 10 fmol/µg (sample B) and 2.5 fmol/µg (sample A) HeLa digest samples. The expected value was 2 (dotted line). Within each set of four points, left to right are ABRF-1, -2, -3 and -4, corresponding to the four spike-in proteins.

Methods

Study samples

Samples were prepared using Hela cells that were released from cell culture plates using trypsin. The cells were washed with PBS and cell pellets dispersed in MS-grade water then disrupted by sonication and diluted to a final protein concentration of 1 mg/mL. All digests were carried out using Promega trypsin with overnight incubations at 37 °C in 40 mM TEAB buffer and after reducing the sample with 10 mM DTT and alkylating with 30 mM IAA. Exogenous proteins were solubilized in MS-grade water and quantified from their absorbance spectra using calculated extinction coefficients [24]. Equimolar amounts of the four proteins were combined prior to reduction and alkylation with DTT and IAA then digestion with trypsin. Digests of Hela and the exogenous protein mix were desalted using Oasis HLB (Waters) cartridges with a single step elution in 65 % (volume fraction) acetonitrile. The four exogenous proteins are: beta-D-galactosidase from *Escherichia coli* (Sigma, catalogue number G8511); Protein G from *Streptococcus aureus* (Sigma, catalogue number P4689); Lysozyme from *Gallus gallus* (Sigma, catalogue number L6876) and amyloglucosidase from *Aspergillus niger* (Sigma, catalogue number A7420). The digest of the exogenous proteins was added to the Hela lysate to achieve a concentration of 1 µM for each protein. This stock was diluted with the base HeLa digest to obtain 10, 2.5 or 0 fmol of the added proteins per 1 µg HeLa digest (sample A - 2.5 fmol spike; sample B - 10 fmol spike, sample C was no spike). Standard iRT peptides (Biognosys) were added to the HeLa plus exogenous protein mixtures. The three study samples of HeLa digest with exogenous proteins and iRT peptides were made one time and were aliquoted into 10 µg HeLa digests aliquots in 0.5 mL lo-bind tubes. These were dried by speed-vac and stored at -80 °C until shipped. Shipping was at ambient temperature.

Study advertisement, enrolment, and timeline

Proteomics Research Group (PRG) members designed the study and announced it at the annual ABRF conference in April 2018. The study was also advertised at the annual conference of the American Society of Mass Spectrometry in June 2018. Interested participants contact details were collected via Google Survey and the distribution of samples began in September 2018 with the majority of participants receiving the samples by November 2018. Participating labs were located in 20 countries and 16 US States. The deadline for data return was extended to June 2019 to accommodate requests by some of the participants. Of the 63 participants who received samples, 45 labs returned datasets. Four participants performed multiple methods or acquired data on multiple instruments, resulting in 49 total datasets.

Information given to participants

Each participant received a numerical study ID with the samples. The participants study ID was and is known only to that investigator and to the anonymizer. Documentation with information about study design, sample preparation, data acquisition and deposition was distributed electronically. This information is included in supplementary information (Supplemental File 1), though it has been edited from its original form to remove vendor contact information. The study documentation included suggestions for reconstituting the samples, LC gradient conditions and DIA data acquisition settings for the following platforms: Thermo Fusion and Fusion Lumos, Thermo QE-HFX, Sciex TripleTOF and Waters Xevo G2 XS platforms. Participants were encouraged to request guidance from members of the PRG if their platform was not included in the original guidelines. For those few investigators, a best attempt was made to design methods with approximately the same DIA cycle time. Finally, there were instructions on how to label the acquired data files and to complete and upload a survey that included self-reported metadata. Throughout the process participants were encouraged and given the means to remain anonymous even when securing technical assistance.

PRG suggested sample resuspension and LC conditions

Participants received three dried samples that have been described. Participants using microflow received two complete sets of the three samples. The suggested method was to bring each up in 0.1 % formic acid, but did not specify the volume. It was expected that nanoflow systems would inject 1 to 2 µg on column, whereas microflow systems might require 4 to 8 µg on column. Participants had discretion to decide the appropriate injection amount for their system and to prepare the samples to allow for replicate injections.

Due to the diversity in LC systems and the latitude for participants to use either nano- or micro-flow applications, we relied on participants to design appropriate gradients that fit within basic guidelines. The suggestion for the study was a two-stage linear gradient lasting 110 to 130 min that we designated as the PRG gradient. The following was suggested: equilibration (trap or direct load) followed by a step from 5 to 25 % acetonitrile over 100 min, then 25 to 40 % acetonitrile over 20 min, and finally 40 to 90 % over 10 min. The final plateau could be held for 5 min before returning to 5 % acetonitrile over 1 min followed by re-equilibration. Roughly half, 23 of the 49, of the datasets reportedly used the PRG gradient (23 of 49 datasets), while 19 of the 49 datasets included specific gradient information that was deposited along with raw files on MassIVE. In general, a multi-step two-hour separation was performed by all participants. Participants were blinded to the sample identity so a run order of A, B, C, blank, B, C, A, blank, C, B, A was suggested to minimize systemic bias due to carryover.

PRG suggested DIA conditions

When constructing a DIA experiment the MS2 mass range, number of MS2 windows, MS2 window width and time spent acquiring data all contribute to establishing the instrument's cycle time, which is the time taken to scan all DIA windows one time, and therefore, how many data points are acquired during a peptide's elution peak. For this study, we recommended static MS2 window widths covering 400 to 1200 *m/z*, with a 1 *m/z* overlap. As an example, this means that one window would stop at 420 *m/z* and the next window would start at 419 *m/z*. The majority of participants followed this recommendation (37 of 49 participants), but other strategies were selected by some participants (Table 2). The design of the study would produce a method with a 3.5 s cycle time. We assumed a 30 s peak width at base and, therefore, a 3.5 s cycle would produce between 7 and 10 data points per peak. We were aware that for participants with tighter peaks this would under sample. Overall, the parameters selected by participants largely achieved 3.5 s cycle (Online-only Table 1) as confirmed by evaluation of the window strategies using Skyline 4.2.0.19107 for each SA_R1 raw file for each submission. These are also reported in the windows.txt and windows.png files on MassIVE MSV000086479.

Specifying the instrument data acquisition time was difficult due to the diversity of platforms and instrument types. For example, for trap-based instruments the acquisition time is related to the transient time, AGC target, and max injection time. We provided general recommendations for QE-HFX, Fusion and Fusion Lumos and personalized recommendations for others, where given resolutions, with known transient times, and max injection times could be suggested to achieve a 3.5 s cycle. For non-trap based instruments such as the triple TOF line, it was much easier to specify instrument time since this is part of the method. In general, though, we suggested the following. For the Fusion and Fusion Lumos, 40 windows 21 *m/z* wide at 30 000 resolution or 62 DIA windows 14 *m/z* wide at 15 000 resolution. For the QE-HFX, 40 windows 21 *m/z* wide at 30 000 resolution. For tripleTOFs, 80 DIA windows 11 m/z wide. For specific settings such as max injection time and AGC (for trap based) or collision energy, please see Supplemental File 1.

Participant Actions: The actions and results of participants 3 and 48 will be discussed in detail.

Participant 3 LC and DIA conditions

Participant 3 self-reported 6 to 9 years of LC-MS/MS experience, had performed DIA a couple times, and used a Thermo Fusion Lumos. The three samples were brought up in 20 µL 0.1% (volume fraction) formic acid to approximately 0.5 µg/µL. Peptide mixtures (2 µL injection; approximately 1 µg) were run in the order specified: A, B, C, blank, B, C, A, blank, C, B, A. The analysis was performed using an UltiMate 3000 Nano LC coupled to a Fusion Lumos mass spectrometer (Thermo Fisher Scientific) with a nano-ESI source. A trap/elute setup was used by trapping with a PepMap 100 C18 trap column (75 µm id x 2 cm length; Thermo Fisher Scientific) at 3 µL/min for 10 min with 2 % acetonitrile (volume fraction) and 0.05 % trifluoroacetic acid (volume fraction) followed by separation on an Acclaim PepMap RSLC 2 µm C18 column (75µm id x 25 cm length; Thermo Fisher Scientific) at 40 °C. Peptides were separated along the suggested PRG LC gradient except that the suggested 90 % acetonitrile (volume fraction) was not possible with the mobile phase setup used. Specifically, a 130 min gradient of 5 % to 32 % mobile phase B [80 % acetonitrile (volume fraction), 0.08 % formic acid (volume fraction)] over 100 min followed by a ramp to 50 % mobile phase B over 20 min and lastly to 95 % mobile phase B over 10 min at a flow rate of 300 nL/min.

Instrument acquisition settings for DIA were exactly those suggested for the 62 windows 14 *m/z* width at 15 000 fragment ion scan resolution (Supplemental File 1). Specifically, a default charge of 4 was used, no internal mass calibration was used, the ion funnel RF was 30 %, and full scan resolution of 120 000 (determined at 200 *m/z*), with an ion target value of $1.0x10^6$, and max injection of 20 ms. Full scan data was acquired from 393 to 1200 *m/z* in profile mode. For DIA settings, quad isolation was set at 14 *m/z* and a list of 62 mass centers was used to accomplish the suggested DIA window scheme, starting at 400 *m/z* and ending at 1193 *m/z*. This resulted in 62 DIA windows of 14 *m/z* width with 1 *m/z* overlap on edge of each window (ex. one window would stop at 420 *m/z* and the next would begin at 419 *m/z*). Fragmentation was performed using higher-energy collisional dissociation (HCD) at a normalized collision energy of 32. Fragmentation profile data was collected from 200 to 2000 *m/z* at 15 000 resolution. The max injection time was 30 ms and an ion target value $1.0x10^6$, and inject parallelizable ions was set to off. Data were acquired under Tune version 2.1 in XCalibur 4.0.

Participant 48 LC and DIA conditions

Participant 48 self-reported >10 years LC-MS/MS experience, expert in DIA, and used a Thermo Fusion Lumos. The three samples were brought up in 20 µL 0.1 % (volume fraction) formic acid to approximately 0.5 µg/µL. Peptide mixtures (approximately 1 µg) were run in the order specified: A, B, C, blank, B, C, A, blank, C, B, A. The analysis was performed using an Nano Acquity (Waters) coupled to a Fusion Lumos mass spectrometer (Thermo Fisher Scientific). A trap/elute setup was used by trapping with a trap column (nanoAcquity Symmetry C18, 5µm, 180 µm x 20 mm) and an analytical column (nanoAcquity BEH C18, 1.7µm, 75µm x 250mm). The outlet of the analytical column was coupled directly to the MS using a Proxeon nanospray source. The peptides were introduced into the mass spectrometer via a PicoTip Emitter 360 µm OD x 20 µm ID; 10 µm tip (New Objective) and a spray voltage of 2.2 kV was applied. The capillary temperature was set at 300 °C. Mobile phase A was water with 0.1 % formic acid (volume fraction) and mobile phase B was acetonitrile with 0.1 % formic acid (volume fraction). The samples were loaded with a constant flow of mobile phase A (5 µL/min) onto the trapping column. Trapping time was 6 minutes. Peptides were eluted via the analytical column with a constant flow of 300 nL/min with the analytical column held at 40 °C. Peptides were separated along the suggested PRG LC gradient (Supplemental File 1).

Instrument acquisition settings for DIA were exactly those suggested for the 40 windows 21 m/z width at 30 000 fragment ion scan resolution (Supplemental File 1). Specifically, a default charge of 4 was used, internal mass calibration was used, the ion funnel RF was 30 %, and full scan resolution of 120

000 (determined at 200 *m/z*), with an ion target value of $1.0x10^6$, and max injection of 20 ms. Full scan data was acquired from 399 to 1200 m/z in profile mode. For DIA settings, quad isolation was set at 21 *m/z* and a list of 40 mass centers were used to accomplish the suggested DIA window scheme, starting at 409.5 *m/z* (center mass) and ending at 1189.5 *m/z* (center mass). This resulted in 40 DIA windows of 21 *m/z* width with 1 *m/z* overlap on the edge of each window. Fragmentation was performed using higher-energy collisional dissociation (HCD) at a normalized collision energy of 30. Profile data was collected from 200 to 2000 *m/z* at 30 000 resolution. The max injection time was 60 ms and an ion target value $1.0x10^6$, and inject parallelizable ions was set to True. Data were acquired under Tune version 2.1 in XCalibur 4.0.

Participant 3 DDA and gas-phase fractionation runs

Participant 3 also performed additional analyses in order to provide data used for constructing spectral and chromatogram libraries. The remaining amounts (approximately 12 µL) of samples A (2.5 fmol spike) and B (10 fmol spike) were combined to obtain a solution that contained the spiked in proteins at approximately 6 fmol spike per µg HeLa digest. The same conditions were used as specified for DIA including the amount of sample injected and the gradient used. Data-acquisition settings were changed to standard DDA. For the data-dependent acquisition (DDA) runs, the Fusion Lumos was operated in positive polarity and data-dependent mode (topN, 3 s cycle time) with a dynamic exclusion of 60 s (with 10 ppm error). Full scan resolution using the orbitrap was set at 120 000 and the mass range was set to 375 to 1500 *m/z* collected in profile mode. Full scan ion target value was $4.0x10^5$ allowing a maximum injection time of 50 ms. Monoisotopic peak determination was used, specifying peptides and an intensity threshold of $1.0x10^4$ was used for precursor selection. Data-dependent fragmentation was performed using higher-energy collisional dissociation (HCD) at a normalized collision energy of 32 with quadrupole isolation at 0.7 *m/z* width. The fragment scan resolution using the orbitrap was set at 30 000, 110 *m/z* as the first mass, ion target value of $2.0x10^5$ and 60 ms maximum injection time and data type set to centroid.

To enable chromatogram library construction, "gas-phase fractionation" was performed[25]. The same injection volume and gradient were used. Five successive runs were performed using a staggered window approach described in detail by Searle *et al*.[25] Briefly, a series of non-overlapping 4 *m/z* wide DIA windows are collected over a short enough mass range to maintain a reasonable DIA cycle. Then the cycle repeats but off-set by 2 *m/z*. This is repeated multiple times so that the full desired precursor mass range was covered. In the case of participant 3, there were five runs each with 2-cycles of 40 windows that were 4 *m/z* wide (detailed in Searle *et al.*[25]). The first run went 400 to 560 *m/z* then 398 to 558 *m/z*. The next four runs were 560 to 720 *m/z*, 720 to 880 *m/z*, 880 to 1040 *m/z* and 1040 to 1200 *m/z*. The raw file names were *TW1, *TW2, *TW3, *TW4, *TW5, respectively, shorthand for tight-window. For each run the instrument specifics were as follows: The Fusion Lumos was operated in positive polarity and no full scan data were acquired. Fragmentation was performed using higher-energy collisional dissociation (HCD) at a normalized collision energy of 32 with quadrupole isolation at 4 *m/z* width in conjunction with the two lists of 40 window centers. Fragment scan resolution using the orbitrap was set at 30 000 and the mass range was set to 200 to 2000 *m/z* collected in profile mode. The default charge was 4, RF lens was 30 % and the ion target value was $1.0x10^6$ allowing a maximum injection time of 60 ms.

Participant 48 DDA runs (Lumos and QE)

Participant 48 also acquired additional data for library construction. The remaining parts of samples A (2.5 fmol spike) and B (10 fmol spike) were combined to obtain a solution that was approximately 6 fmol spike per µg HeLa digest. The same conditions were used as specified for DIA, including 1 µg injection and the same gradient, with the main change being data-acquisition settings. For the data-

dependent acquisition runs, the Fusion Lumos was operated in positive polarity and data-dependent mode (topN, 3 s cycle time) with a dynamic exclusion of 15 s (with 10 ppm error). Full scan resolution using the orbitrap was set at 60 000 and the mass range was set to 375 to 1500 *m/z* collected in profile mode. Full scan ion target value was $2.0x10^5$ allowing a maximum injection time of 50 ms. Monoisotopic peak determination was used, specifying peptides and an intensity threshold of $5.0x10^4$ was used for precursor selection. Only multiply charged (2+ to 7+) precursor ions were selected for fragmentation. Isotopes were excluded. Data-dependent fragmentation was performed using higher-energy collisional dissociation (HCD) at a normalized collision energy of 30 with quadrupole isolation at 1.4 *m/z* width. The fragment scan resolution using the orbitrap was set at 15 000, 120 *m/z* as the first mass, ion target value of $2.0x10^5$ and 22 ms maximum injection time and data type set to centroid.

Participant 48 also performed additional analyses of the spike-in proteins alone to be included as a library when the data was searched against the Pan-Human library[26]. Participant 48 was supplied with a tryptic digest of approximately 16.9 pmol of each protein. The sample was resuspended in 170 µL (approx. 100 fmol/µL), the iRT kit added, and four injections were made in DDA and DIA, respectively, with the amount on column ranging from 100 fmol to 800 fmol (100, 200, 400, 800). These DDA and DIA runs of the spike-in proteins are described below.

The same conditions were used for the LC, with the exception that the nanoUPLC hardware was an M-Class NanoAcquity from Waters. The same gradient was applied (two-step PRG recommended), with the main change being the MS instrument settings for the QE-HFX (Thermo). For the data-dependent acquisition runs, the QE-HFX was operated in positive polarity and data-dependent mode (top15) with a dynamic exclusion of 20 s (with 10 ppm error). Full scan resolution using the orbitrap was set at 60 000 and the mass range was set to 350 to 1650 *m/z* collected in profile mode. Full scan ion target value was $3.0x10^6$ allowing a maximum injection time of 20 ms. Peptide setting was set to "preferred" and an intensity threshold of $1.0x10^4$ was used for precursor selection and AGC of $1.0x10^3$. Only multiply charged (2+ to 5+) precursor ions were selected for fragmentation. Isotopes were excluded. Data-dependent fragmentation was performed using higher-energy collisional dissociation (HCD) at a normalized collision energy of 27 with quadrupole isolation at 1.6 *m/z* width. The fragment scan resolution using the orbitrap was set at 15 000, 120 *m/z* as the first mass, ion target value of $2.0x10^5$ and 25 ms maximum injection time and data type set to profile. The default charge state was set to 2+. Data were acquired under Tune version 2.9 in XCalibur 4.0.

For the data independent acquisition runs, the same conditions as for the DDA were applied to the LC gradient. The following parameters were different for the QE-HFX acquisition: MS1 full scans were acquired using the orbitrap resolution set at 120 000 and the mass range was set to 400 to 1200 *m/z* and data were collected in profile mode. Full scan ion target value was $3.0x10^6$ allowing a maximum injection time of 20 ms. Data independent scans were set to 40 fixed windows, each of width 21 *m/z* (the same as for the Lumos DIA by participant 48). A maximum injection time of 60 ms was set with ion target value of $3.0x10^6$. Fragmentation (HCD) for the DIA scans in MS2 was carried out with a normalized collision energy of 30, the first MS2 mass was set to 200 *m/z* and data type set to profile. The default charge state was set to 3+.

Analysis of participant 3 and 48 data

A preliminary analysis of the majority of participants data was presented at the ABRF 2019 meeting and is available for reference[27]. Herein we describe the analysis of two participants using Spectronaut (v13.6.190905.43655; Biognosys AG)[28] and Scaffold DIA (v1.3.1; Proteome Software). Spectronaut and Scaffold DIA are two of the many available software packages capable of DIA analysis. They were selected for this project due to the expertise of the authors. We recommend similar analysis in other programs (see Data Usage), though the settings listed may not necessarily translate. Participants 3 and 48 both performed the replicate analysis of three samples using an Orbitrap Fusion Lumos. They

both collected DDA in replicate of a combined sample, while data of just the digested spike proteins was only collected on a QE-HFX by participant 48. This allowed comparison of different library generation techniques within Spectronaut: directDIA, where only the DIA data is used; DpD, directDIA plus DDA where separate search archives (i.e., libraries) are constructed of the DIA data and the DDA, then combined; Pan-Human plus spikes, where a search archive of the spikes alone was combined with the Pan-Human library[26]. Since only Participant 3 collected data using gas-phase fractionation, this was used for generating a chromatogram library in Scaffold DIA and wasn't utilized for Participant 48's data.

The following settings were used in Spectronaut for directDIA libraries (setting tabs are bold), which can be retrieved as .xls and .kit files on MassIVE MSV000086479 as 03_lumos_directDIA and 48_lumos_directDIA. **Sequences:** Trypsin/P selected, max pep length 52, min pep length 7, two missed cleavages, KR as special amino acids in decoy generation, toggle N-terminal M set to true. **Labelling:** no labelling settings were used. **Applied modifications:** maximum of five variable modifications using fixed carbamidomethyl (C), and variable acetyl (protein N-term) and oxidation (M). **Identification:** per run machine learning, Q-value cut-off of 0.01 for precursors and proteins, single hits defined by stripped sequence, and do not exclude single hit proteins, PTM localization set to true with a probability cut-off of 0.75, kernel density p-value estimator. **Quantification**: interference correction was used with excluding all multi-channel interferences with minimum of 2 and 3 for MS1 and MS2, respectively. Proteotypicity filter was set to none, major protein grouping by protein group ID, minor peptide grouping by stripped sequence, major group quantity set to mean peptide quantity, a Major Group Top N was used (min of 1, max of 3), minor group quantity set to mean precursor quantity, a Minor Group Top N was used (min1, max of 3), quantity MS-level used MS2 area, data filtering by q-value, cross run normalization was used with global median normalization and automatic row selection, no modifications or amino acids were specified, best N fragments per peptide was set to between 3 and 6, with ion charge and type not used. **Workflow:** no workflow was used. **Post Analysis**: no calculated explained TIC or sample correlation matrix, differential abundance grouping using major group (from quantification settings) and smallest quantitative unit defined by precursor ion (from quantification settings), differential abundance was not used for conclusions but the following settings were used in the attached files: Student's t-test, no group-wise testing correction, run clustering was set using the Manhattan distance metric and Ward's method for linkage strategy and runs were ordered by clustering without Z-score transformation. The fasta files used are included in MassIVE MSV000086479, but briefly the UniProtKB Swiss-Prot 2018_06 human database (taxonomy:9606), canonical only was concatenated with the four spike proteins entries [ABRF-1 P00722 beta-galactosidase (*Escherichia coli*), ABRF-2 P00698 lysozyme C (*Gallus gallus*), ABRF-3 P69328 glucoamylase (*Aspergillus niger*), ABRF-4 Q54181 protein G' (*Streptococcus* sp. group G)], the iRT Fusion sequence supplied by Biognosys [LGGNEQVTRYILAGVENSKGTFIIDPGGVIRGTFIIDPAAVIRGAGSS EPVTGLDAKTPVISGGPYEYRVEATFGVDESNAKTPVITGAPYEYRDGLDAASYYAPVRADVTPADFSEWSKLFLQF GAQGSPFLK], and a contaminants database of 247 entries. These two .fasta files are on MassIVE MSV000086479 as sp_human_180620_plus_PRG_ABRF_4_prot.fasta and contaminants_ 20120713.fasta, respectively.

For DpD approaches, the DDA data was used to generate a search archive with Pulsar using the same settings described for directDIA and the resulting search archive was combined with a library made directly from the DIA data using the settings described above. There were three DpD libraries created: each participant individually, then a combined library. These are included as 03_lumos_DpD, 48_lumos_DpD, and 03_lumos_48_lumos_DpD as .xls and .kit, on MassIVE MSV000086479. The Pan-Human search archive was downloaded within Spectronaut and is also available as Pan Human Library – ETH .xls and .kit on MassIVE MSV000086479. This was combined with a directDIA plus DDA library of digested spike proteins and is on MassIVE MSV000086479 as 48_qehfx_spikes_DpD .xls and .kit.

When searching with the DpD search archives or the Pan-Human derived archive, the following settings were used: **Data extraction:** maximum intensity extraction for MS1 and MS2, dynamic MS1 mass tolerance strategy with a correlation factor of 1, and a dynamic MS2 mass tolerance strategy with a correction of 1. **XIC extraction:** a dynamic XIC RT extraction window was used with a correction factor of 1. **Calibration:** allowed source specific iRT calibration with an automatic calibration mode, used a maximum intensity MZ extraction strategy, precision iRT was set to true with excluded deamidated peptides and a local (non-linear) iRT<->RT regression type, used Biognosys iRT kit, and no calibration carry-over. **Identification:** same settings as used in directDIA. **Quantification:** same as in directDIA. **Workflow:** no *in silico* library optimization, multi-channel workflow definition from library annotation with a fallback option as labelled, and no profiling or unify peptide peaks strategy was used. **Protein inference:** automatic. **Post analysis:** same settings as used in directDIA.

Since participant 3 also collected gas-phase fractionation data (described above), this DIA data was also processed in Scaffold DIA (v1.3.1) three different ways: (1) by creating a chromatogram library using only the gas-phase fractionation data, (2) using these data combined with the Pan-Human library and (3) using these data combined with a Prosit *in silico* library. The Pan-Human library was converted directly using EncyclopeDIA (v0.8.1)[25] from phl004_canonical_sall_osw.csv, downloaded from the SwathAtlas repository (https://db.systemsbiology.net/sbeams/cgi/PeptideAtlas/GetDIALibs). The Prosit predictions used the EncyclopeDIA library generation defaults[20]. These defaults were predictions for +2H/+3H peptides between 396.4 and 1002.7 m/z with up to 1 missed cleavage. The NCE setting was 33, assuming all peptides were fragmented in DIA as +2H peptides. The additional four ABRF peptides were predicted using the same pipeline, but for all +2H/+3H/+4H/+5H peptides between 396.4 and 1002.7 *m/z* with up to 2 missed cleavage. Again, the NCE setting was 33, assuming all peptides were fragmented in DIA as +2H peptides. The resulting library files for Pan-Human and Prosit human plus PRG spike proteins can be found on MassIVE MSV000086479 as combined_prg_pan_human.dlib and combined_prg_sprothuman.dlib, respectively.

All raw data files were converted to mzML format (within Scaffold DIA) using ProteoWizard (v3.0.18342)[29]. In the first case where an external library was not used, the reference spectral library was created by EncyclopeDIA (v0.8.1)[25]. Reference samples were individually searched against the same fasta described above, with a peptide mass tolerance of 10.0 ppm and a fragment mass tolerance of 10.0 ppm. Fixed modifications considered were: Carbamidomethylation C. In the second case, when combining the data with the Pan-human library, the reference spectral library files were individually searched against a combined fasta and the dlib with a peptide mass tolerance of 10.0 ppm and a fragment mass tolerance of 10.0 ppm. Variable modifications considered were: Oxidation M and Carbamidomethylation C (since these are used in the Pan-Human library). In the third case, when combining the data with Prosit predictions, the reference spectral library files were individually searched against a combined fasta and the dlib with a peptide mass tolerance of 10.0 ppm and a fragment mass tolerance of 10.0 ppm. Variable modifications considered were: Carbamidomethylation C.

For all three search approaches the digestion enzyme was assumed to be trypsin with a maximum of 1 missed cleavage site allowed. Only peptides with charges in the range +2 to +3 and length in the range 6 to 30 were considered. Peptides identified in each search were filtered by Percolator (v3.01.nightly-13-655e4c7-dirty)[30-32] to achieve a maximum FDR of 0.01. Individual search results were combined and peptides were again filtered to an FDR threshold of 0.01 for inclusion in the reference library.

Analytical samples (i.e., the replicate injections of the three ABRF samples participant 3 analyzed), were aligned based on retention times and individually searched against 03 Chromatogram Library.elib, 03 - PH plus CL library.elib or 03 - Prosit plus CL library.elib (created as described above

and available on MassIVE MSV000086479) with search settings identical to those used to create the reference library. Peptide quantification was performed by EncyclopeDIA (v0.8.1)[25]. For each peptide, the five highest quality fragment ions were selected for quantitation. Proteins that contained similar peptides and could not be differentiated based on MS/MS analysis were grouped to satisfy the principles of parsimony. Proteins with a minimum of two identified peptides were thresholded to achieve a protein FDR threshold of 1.0 %. These files are available as 03 - CL only.sdia, 03 - PH plus CL.sdia and 03 - Prosit plus CL.sdia.

For all approaches, intensity values of the four spike-in proteins were used to compare relative quantification between the different approaches. Specifically, Sample A versus Sample B was used to evaluate how well each approach measured the predicted 4-fold difference in protein concentration. To easily calculate the 95% confidence interval of each fold-change the topTable function within the limma package (v3.40.6)[33] in R (v3.6.0; 64-bit) was used with the argument "confint=TRUE". To accomplish this, first exported intensity values were transformed to log2 values and this matrix was used with limma. A summary figure outlining the workflow for the data from participants 3 and 48 is shown in Figure 4.

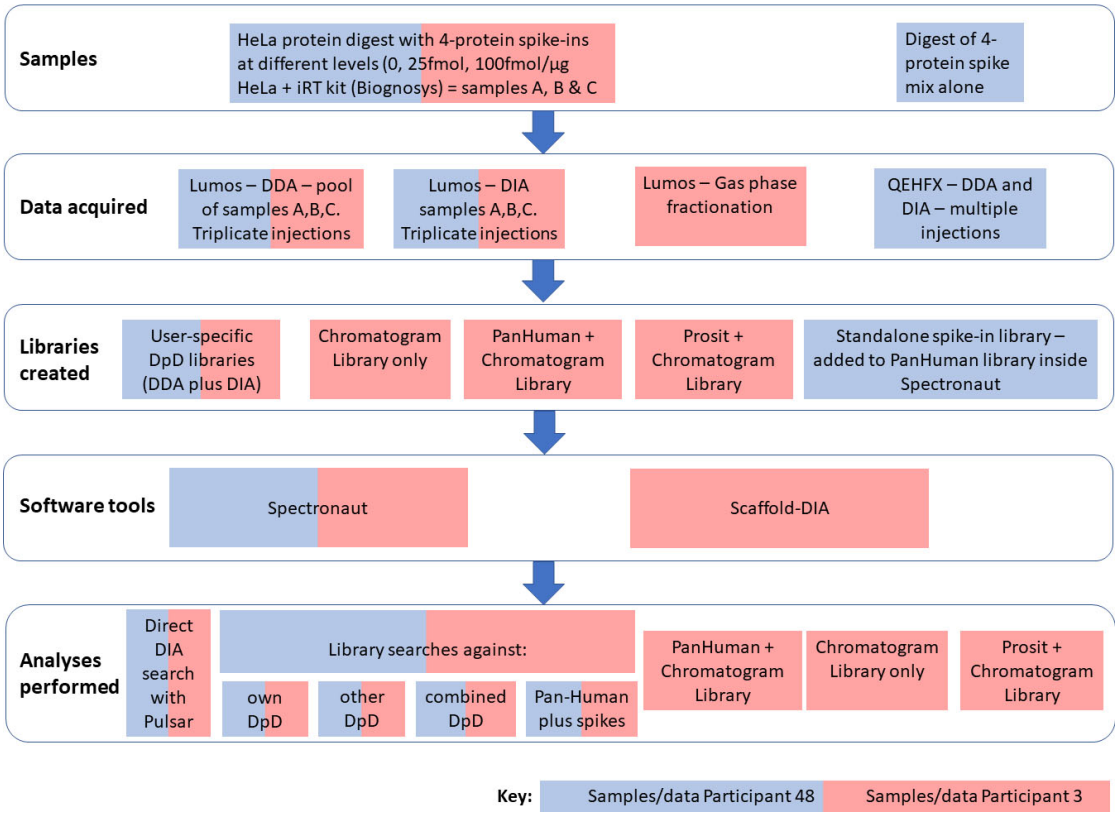

Figure 4. Summary flowchart showing steps taken from samples assigned to participants 3 and 48.

Data Records

Sample	Replicate	Participant	Data Type	Data
SA	R1	01	DIA_Data	01_qehfx_lab_SA_R1.raw
SA	R2	01	DIA_Data	01_qehfx_lab_SA_R2.raw
SA	R3	01	DIA_Data	01_qehfx_lab_SA_R3.raw
SB	R1	01	DIA_Data	01_qehfx_lab_SB_R1.raw
SB	R2	01	DIA_Data	01_qehfx_lab_SB_R2.raw
SB	R3	01	DIA_Data	01_qehfx_lab_SB_R3.raw
SC	R1	01	DIA_Data	01_qehfx_lab_SC_R1.raw
SC	R2	01	DIA_Data	01_qehfx_lab_SC_R2.raw
SC	R3	01	DIA_Data	01_qehfx_lab_SC_R3.raw
		01	windows.png	01_windows.png
		01	windows.txt	01_windows.txt
		03	instrument_method	03_lumos_156min_15kMS2_62_14mz.meth
SA	R1	03	DIA_Data	03_lumos_prg_SA_R1.raw
SA	R2	03	DIA_Data	03_lumos_prg_SA_R2.raw
SA	R3	03	DIA_Data	03_lumos_prg_SA_R3.raw
SB	R1	03	DIA_Data	03_lumos_prg_SB_R1.raw
SB	R2	03	DIA_Data	03_lumos_prg_SB_R2.raw
SB	R3	03	DIA_Data	03_lumos_prg_SB_R3.raw
SC	R1	03	DIA_Data	03_lumos_prg_SC_R1.raw
SC	R2	03	DIA_Data	03_lumos_prg_SC_R2.raw
SC	R3	03	DIA_Data	03_lumos_prg_SC_R3.raw
		03	windows.png	03_windows.png
		03	windows.txt	03_windows.txt
		04	CustomMSMethod.csv	04_CustomMSMethod.csv
SA	R1	04	DIA_Data	04_orbive_lab_SA_R1.raw
SA	R2	04	DIA_Data	04_orbive_lab_SA_R2.raw
SA	R3	04	DIA_Data	04_orbive_lab_SA_R3.raw
SB	R1	04	DIA_Data	04_orbive_lab_SB_R1.raw
SB	R2	04	DIA_Data	04_orbive_lab_SB_R2.raw
SB	R3	04	DIA_Data	04_orbive_lab_SB_R3.raw
SC	R1	04	DIA_Data	04_orbive_lab_SC_R1.raw
SC	R2	04	DIA_Data	04_orbive_lab_SC_R2.raw
SC	R3	04	DIA_Data	04_orbive_lab_SC_R3.raw
		04	windows.png	04_windows.png
		04	windows.txt	04_windows.txt
		05	CustomLCMethod.csv	05_CustomLCMethod.csv
		05	CustomMSMethod.csv	05_CustomMSMethod.csv
SA	R1	05	DIA_Data	05_lumos_lab_SA_R1.raw
SA	R2	05	DIA_Data	05_lumos_lab_SA_R2.raw
SA	R3	05	DIA_Data	05_lumos_lab_SA_R3.raw
SB	R1	05	DIA_Data	05_lumos_lab_SB_R1.raw
SB	R2	05	DIA_Data	05_lumos_lab_SB_R2.raw
SB	R3	05	DIA_Data	05_lumos_lab_SB_R3.raw
SC	R1	05	DIA_Data	05_lumos_lab_SC_R1.raw

SC	R2	05	DIA_Data	05_lumos_lab_SC_R2.raw
SC	R3	05	DIA_Data	05_lumos_lab_SC_R3.raw
		05	windows.png	05_windows.png
		05	windows.txt	05_windows.txt
SA	R1	06	DIA_Data	06_lumos_lab_SA_R1.raw
SA	R2	06	DIA_Data	06_lumos_lab_SA_R2.raw
SA	R3	06	DIA_Data	06_lumos_lab_SA_R3.raw
SB	R1	06	DIA_Data	06_lumos_lab_SB_R1.raw
SB	R2	06	DIA_Data	06_lumos_lab_SB_R2.raw
SB	R3	06	DIA_Data	06_lumos_lab_SB_R3.raw
SC	R1	06	DIA_Data	06_lumos_lab_SC_R1.raw
SC	R2	06	DIA_Data	06_lumos_lab_SC_R2.raw
SC	R3	06	DIA_Data	06_lumos_lab_SC_R3.raw
		06	06_windows.png	06_windows.png
		06	06_windows.txt	06_windows.txt
SA	R1	07	DIA_Data	07_fusion_prg15k_SA_R1.raw
SA	R2	07	DIA_Data	07_fusion_prg15k_SA_R2.raw
SA	R3	07	DIA_Data	07_fusion_prg15k_SA_R3.raw
SB	R1	07	DIA_Data	07_fusion_prg15k_SB_R1.raw
SB	R2	07	DIA_Data	07_fusion_prg15k_SB_R2.raw
SB	R3	07	DIA_Data	07_fusion_prg15k_SB_R3.raw
SC	R1	07	DIA_Data	07_fusion_prg15k_SC_R1.raw
SC	R2	07	DIA_Data	07_fusion_prg15k_SC_R2.raw
SC	R3	07	DIA_Data	07_fusion_prg15k_SC_R3.raw
SA	R1	07	DIA_Data	07_fusion_prg30k_SA_R1.raw
SA	R3	07	DIA_Data	07_fusion_prg30k_SA_R3.raw
SB	R2	07	DIA_Data	07_fusion_prg30k_SB_R2.raw
SB	R3	07	DIA_Data	07_fusion_prg30k_SB_R3.raw
SC	R1	07	DIA_Data	07_fusion_prg30k_SC_R1.raw
SC	R2	07	DIA_Data	07_fusion_prg30k_SC_R2.raw
SC	R3	07	DIA_Data	07_fusion_prg30k_SC_R3.raw
		07	DIA_Data	07_windows_15k.png
		07	DIA_Data	07_windows_15k.txt
		07	DIA_Data	07_windows_30k.png
		07	DIA_Data	07_windows_30k.txt
SA	R1	08	DIA_Data	08_fusion_prg_SA_R1.raw
SA	R2	08	DIA_Data	08_fusion_prg_SA_R2.raw
SA	R3	08	DIA_Data	08_fusion_prg_SA_R3.raw
SB	R1	08	DIA_Data	08_fusion_prg_SB_R1.raw
SB	R2	08	DIA_Data	08_fusion_prg_SB_R2.raw
SB	R3	08	DIA_Data	08_fusion_prg_SB_R3.raw
SC	R1	08	DIA_Data	08_fusion_prg_SC_R1.raw
SC	R2	08	DIA_Data	08_fusion_prg_SC_R2.raw
SC	R3	08	DIA_Data	08_fusion_prg_SC_R3.raw
		08	windows.png	08_windows.png
		08	windows.txt	08_windows.txt

SA	R1	10	DIA_Data	10_qehf_prg_SA_R1.raw
SA	R2	10	DIA_Data	10_qehf_prg_SA_R2.raw
SA	R3	10	DIA_Data	10_qehf_prg_SA_R3.raw
SB	R1	10	DIA_Data	10_qehf_prg_SB_R1.raw
SB	R2	10	DIA_Data	10_qehf_prg_SB_R2.raw
SB	R3	10	DIA_Data	10_qehf_prg_SB_R3.raw
SC	R1	10	DIA_Data	10_qehf_prg_SC_R1.raw
SC	R2	10	DIA_Data	10_qehf_prg_SC_R2.raw
SC	R3	10	DIA_Data	10_qehf_prg_SC_R3.raw
		10	windows.png	10_windows.png
		10	windows.txt	10_windows.txt
SA	R1	13	DIA_Data	13_fusion_prg_SA_R1.raw
SA	R2	13	DIA_Data	13_fusion_prg_SA_R2.raw
SA	R3	13	DIA_Data	13_fusion_prg_SA_R3.raw
SB	R1	13	DIA_Data	13_fusion_prg_SB_R1.raw
SB	R2	13	DIA_Data	13_fusion_prg_SB_R2.raw
SB	R3	13	DIA_Data	13_fusion_prg_SB_R3.raw
SC	R1	13	DIA_Data	13_fusion_prg_SC_R1.raw
SC	R2	13	DIA_Data	13_fusion_prg_SC_R2.raw
SC	R3	13	DIA_Data	13_fusion_prg_SC_R3.raw
		13	windows.png	13_windows.png
		13	windows.txt	13_windows.txt
		14	CustomLCMethod.csv	14_CustomLCMethod.csv
		14	CustomMSMethod.csv	14_CustomMSMethod.csv
SA	R1	14	DIA_Data	14_tt6600_lab_SA_R1.wiff
SA	R1	14	DIA_Data	14_tt6600_lab_SA_R1.wiff.scan
SA	R2	14	DIA_Data	14_tt6600_lab_SA_R2.wiff
SA	R2	14	DIA_Data	14_tt6600_lab_SA_R2.wiff.scan
SA	R3	14	DIA_Data	14_tt6600_lab_SA_R3.wiff
SA	R3	14	DIA_Data	14_tt6600_lab_SA_R3.wiff.scan
SB	R1	14	DIA_Data	14_tt6600_lab_SB_R1.wiff
SB	R1	14	DIA_Data	14_tt6600_lab_SB_R1.wiff.scan
SB	R2	14	DIA_Data	14_tt6600_lab_SB_R2.wiff
SB	R2	14	DIA_Data	14_tt6600_lab_SB_R2.wiff.scan
SB	R3	14	DIA_Data	14_tt6600_lab_SB_R3.wiff
SB	R3	14	DIA_Data	14_tt6600_lab_SB_R3.wiff.scan
SC	R1	14	DIA_Data	14_tt6600_lab_SC_R1.wiff
SC	R1	14	DIA_Data	14_tt6600_lab_SC_R1.wiff.scan
SC	R2	14	DIA_Data	14_tt6600_lab_SC_R2.wiff
SC	R2	14	DIA_Data	14_tt6600_lab_SC_R2.wiff.scan
SC	R3	14	DIA_Data	14_tt6600_lab_SC_R3.wiff
SC	R3	14	DIA_Data	14_tt6600_lab_SC_R3.wiff.scan
		14	windows.png	14_windows.png
		14	windows.txt	14_windows.txt
		15	CustomLCMethod.csv	15_CustomLCMethod.csv
		15	CustomMSMethod.csv	15_CustomMSMethod.csv

SA	R1	15	DIA_Data	15_orbielite_lab_SA_R1.raw
SA	R2	15	DIA_Data	15_orbielite_lab_SA_R2.raw
SA	R3	15	DIA_Data	15_orbielite_lab_SA_R3.raw
SC	R1	15	DIA_Data	15_orbielite_lab_SC_R1.raw
SC	R2	15	DIA_Data	15_orbielite_lab_SC_R2.raw
SC	R3	15	DIA_Data	15_orbielite_lab_SC_R3.raw
		15	windows.png	15_windows.png
		15	windows.txt	15_windows.txt
SA	R1	16	DIA_Data	16_tt6600_prg_SA_R1.wiff
SA	R1	16	DIA_Data	16_tt6600_prg_SA_R1.wiff.scan
SA	R2	16	DIA_Data	16_tt6600_prg_SA_R2.wiff
SA	R2	16	DIA_Data	16_tt6600_prg_SA_R2.wiff.scan
SA	R3	16	DIA_Data	16_tt6600_prg_SA_R3.wiff
SA	R3	16	DIA_Data	16_tt6600_prg_SA_R3.wiff.scan
SB	R1	16	DIA_Data	16_tt6600_prg_SB_R1.wiff
SB	R1	16	DIA_Data	16_tt6600_prg_SB_R1.wiff.scan
SB	R2	16	DIA_Data	16_tt6600_prg_SB_R2.wiff
SB	R2	16	DIA_Data	16_tt6600_prg_SB_R2.wiff.scan
SB	R3	16	DIA_Data	16_tt6600_prg_SB_R3.wiff
SB	R3	16	DIA_Data	16_tt6600_prg_SB_R3.wiff.scan
SC	R1	16	DIA_Data	16_tt6600_prg_SC_R1.wiff
SC	R1	16	DIA_Data	16_tt6600_prg_SC_R1.wiff.scan
SC	R2	16	DIA_Data	16_tt6600_prg_SC_R2.wiff
SC	R2	16	DIA_Data	16_tt6600_prg_SC_R2.wiff.scan
SC	R3	16	DIA_Data	16_tt6600_prg_SC_R3.wiff
SC	R3	16	DIA_Data	16_tt6600_prg_SC_R3.wiff.scan
		16	windows.png	16_windows.png
		16	windows.txt	16_windows.txt
SA	R1	17	DIA_Data	17_qehfx_prg_SA_R1.raw
SA	R2	17	DIA_Data	17_qehfx_prg_SA_R2.raw
SA	R3	17	DIA_Data	17_qehfx_prg_SA_R3.raw
SB	R1	17	DIA_Data	17_qehfx_prg_SB_R1.raw
SB	R2	17	DIA_Data	17_qehfx_prg_SB_R2.raw
SB	R3	17	DIA_Data	17_qehfx_prg_SB_R3.raw
SC	R1	17	DIA_Data	17_qehfx_prg_SC_R1.raw
SC	R2	17	DIA_Data	17_qehfx_prg_SC_R2.raw
SC	R3	17	DIA_Data	17_qehfx_prg_SC_R3.raw
		17	windows.png	17_windows.png
		17	windows.txt	17_windows.txt
		18	CustomLCMethod.csv	18_CustomLCMethod.csv
SA	R1	18	DIA_Data	18_fusion_prg_SA_R1.raw
SA	R2	18	DIA_Data	18_fusion_prg_SA_R2.raw
SA	R3	18	DIA_Data	18_fusion_prg_SA_R3.raw
SB	R1	18	DIA_Data	18_fusion_prg_SB_R1.raw
SB	R2	18	DIA_Data	18_fusion_prg_SB_R2.raw
SB	R3	18	DIA_Data	18_fusion_prg_SB_R3.raw

SC	R1	18	DIA_Data	18_fusion_prg_SC_R1.raw
SC	R2	18	DIA_Data	18_fusion_prg_SC_R2.raw
SC	R3	18	DIA_Data	18_fusion_prg_SC_R3.raw
		18	windows.png	18_windows.png
		18	windows.txt	18_windows.txt
		19	CustomLCMethod.csv	19_CustomLCMethod.csv
		19	CustomMSMethod.csv	19_CustomMSMethod.csv
SA	R2	19	DIA_Data	19_qehfx_lab_SA_R2.raw
SA	R3	19	DIA_Data	19_qehfx_lab_SA_R3.raw
SB	R1	19	DIA_Data	19_qehfx_lab_SB_R1.raw
SB	R2	19	DIA_Data	19_qehfx_lab_SB_R2.raw
SB	R3	19	DIA_Data	19_qehfx_lab_SB_R3.raw
SC	R1	19	DIA_Data	19_qehfx_lab_SC_R1.raw
SC	R2	19	DIA_Data	19_qehfx_lab_SC_R2.raw
SC	R3	19	DIA_Data	19_qehfx_lab_SC_R3.raw
		19	windows.png	19_windows.png
		19	windows.txt	19_windows.txt
		20	CustomLCmethod.csv	20_CustomLCmethod.csv
		20	CustomMSmethod.csv	20_CustomMSmethod.csv
		20	instrument_method	20_PRG2018_SWATH.dam
SA	R1	20	DIA_Data	20_tt5600_lab_SA_R1.wiff
SA	R1	20	DIA_Data	20_tt5600_lab_SA_R1.wiff.scan
SA	R2	20	DIA_Data	20_tt5600_lab_SA_R2.wiff
SA	R2	20	DIA_Data	20_tt5600_lab_SA_R2.wiff.scan
SA	R3	20	DIA_Data	20_tt5600_lab_SA_R3.wiff
SA	R3	20	DIA_Data	20_tt5600_lab_SA_R3.wiff.scan
SB	R1	20	DIA_Data	20_tt5600_lab_SB_R1.wiff
SB	R1	20	DIA_Data	20_tt5600_lab_SB_R1.wiff.scan
SB	R2	20	DIA_Data	20_tt5600_lab_SB_R2.wiff
SB	R2	20	DIA_Data	20_tt5600_lab_SB_R2.wiff.scan
SB	R3	20	DIA_Data	20_tt5600_lab_SB_R3.wiff
SB	R3	20	DIA_Data	20_tt5600_lab_SB_R3.wiff.scan
SC	R1	20	DIA_Data	20_tt5600_lab_SC_R1.wiff
SC	R1	20	DIA_Data	20_tt5600_lab_SC_R1.wiff.scan
SC	R2	20	DIA_Data	20_tt5600_lab_SC_R2.wiff
SC	R2	20	DIA_Data	20_tt5600_lab_SC_R2.wiff.scan
SC	R3	20	DIA_Data	20_tt5600_lab_SC_R3.wiff
SC	R3	20	DIA_Data	20_tt5600_lab_SC_R3.wiff.scan
		20	windows.png	20_windows.png
		20	windows.txt	20_windows.txt
		21	CustomLCMethod.csv	21_CustomLCMethod.csv
SA	R1	21	DIA_Data	21_fusion_prg_SA_R1.raw
SA	R2	21	DIA_Data	21_fusion_prg_SA_R2.raw
SA	R3	21	DIA_Data	21_fusion_prg_SA_R3.raw
SB	R1	21	DIA_Data	21_fusion_prg_SB_R1.raw
SB	R2	21	DIA_Data	21_fusion_prg_SB_R2.raw

SB	R3	21	DIA_Data	21_fusion_prg_SB_R3.raw
SC	R1	21	DIA_Data	21_fusion_prg_SC_R1.raw
SC	R2	21	DIA_Data	21_fusion_prg_SC_R2.raw
SC	R3	21	DIA_Data	21_fusion_prg_SC_R3.raw
		21	windows.png	21_windows.png
		21	windows.txt	21_windows.txt
		23	CustomLCMethod.csv	23_CustomLCMethod.csv
SA	R1	23	DIA_Data	23_xevo_prg_SA_R1.raw
SA	R2	23	DIA_Data	23_xevo_prg_SA_R2.raw
SA	R3	23	DIA_Data	23_xevo_prg_SA_R3.raw
SB	R1	23	DIA_Data	23_xevo_prg_SB_R1.raw
SB	R2	23	DIA_Data	23_xevo_prg_SB_R2.raw
SB	R3	23	DIA_Data	23_xevo_prg_SB_R3.raw
SC	R1	23	DIA_Data	23_xevo_prg_SC_R1.raw
SC	R2	23	DIA_Data	23_xevo_prg_SC_R2.raw
SC	R3	23	DIA_Data	23_xevo_prg_SC_R3.raw
SA	R2	25	DIA_Data	25_fusion_prg_SA_R2.raw
SA	R3	25	DIA_Data	25_fusion_prg_SA_R3.raw
SB	R1	25	DIA_Data	25_fusion_prg_SB_R1.raw
SB	R2	25	DIA_Data	25_fusion_prg_SB_R2.raw
SB	R3	25	DIA_Data	25_fusion_prg_SB_R3.raw
SC	R1	25	DIA_Data	25_fusion_prg_SC_R1.raw
SC	R2	25	DIA_Data	25_fusion_prg_SC_R2.raw
SC	R3	25	DIA_Data	25_fusion_prg_SC_R3.raw
		25	windows.png	25_windows.png
		25	windows.txt	25_windows.txt
		26	CustomLCMethod.csv	26_CustomLCMethod.csv
		26	CustomMSMethod.csv	26_CustomMSMethod.csv
SA	R1	26	DIA_Data	26_tt5600_lab_SA_R1.wiff
SA	R1	26	DIA_Data	26_tt5600_lab_SA_R1.wiff.scan
SA	R2	26	DIA_Data	26_tt5600_lab_SA_R2.wiff
SA	R2	26	DIA_Data	26_tt5600_lab_SA_R2.wiff.scan
SA	R3	26	DIA_Data	26_tt5600_lab_SA_R3.wiff
SA	R3	26	DIA_Data	26_tt5600_lab_SA_R3.wiff.scan
SB	R1	26	DIA_Data	26_tt5600_lab_SB_R1.wiff
SB	R1	26	DIA_Data	26_tt5600_lab_SB_R1.wiff.scan
SB	R2	26	DIA_Data	26_tt5600_lab_SB_R2.wiff
SB	R2	26	DIA_Data	26_tt5600_lab_SB_R2.wiff.scan
SB	R3	26	DIA_Data	26_tt5600_lab_SB_R3.wiff
SB	R3	26	DIA_Data	26_tt5600_lab_SB_R3.wiff.scan
SC	R1	26	DIA_Data	26_tt5600_lab_SC_R1.wiff
SC	R1	26	DIA_Data	26_tt5600_lab_SC_R1.wiff.scan
SC	R2	26	DIA_Data	26_tt5600_lab_SC_R2.wiff
SC	R2	26	DIA_Data	26_tt5600_lab_SC_R2.wiff.scan
SC	R3	26	DIA_Data	26_tt5600_lab_SC_R3.wiff
SC	R3	26	DIA_Data	26_tt5600_lab_SC_R3.wiff.scan

		26	windows.png	26_windows.png
		26	windows.txt	26_windows.txt
SA	R1	28	DIA_Data	28_qehf_prg_SA_R1.raw
SA	R2	28	DIA_Data	28_qehf_prg_SA_R2.raw
SA	R3	28	DIA_Data	28_qehf_prg_SA_R3.raw
SB	R1	28	DIA_Data	28_qehf_prg_SB_R1.raw
SB	R2	28	DIA_Data	28_qehf_prg_SB_R2.raw
SB	R3	28	DIA_Data	28_qehf_prg_SB_R3.raw
SC	R1	28	DIA_Data	28_qehf_prg_SC_R1.raw
SC	R2	28	DIA_Data	28_qehf_prg_SC_R2.raw
SC	R3	28	DIA_Data	28_qehf_prg_SC_R3.raw
		28	windows.png	28_windows.png
		28	windows.txt	28_windows.txt
SA	R1	29	DIA_Data	29_lumos_SA_R1.raw
SA	R2	29	DIA_Data	29_lumos_SA_R2.raw
SA	R3	29	DIA_Data	29_lumos_SA_R3.raw
SB	R1	29	DIA_Data	29_lumos_SB_R1.raw
SB	R2	29	DIA_Data	29_lumos_SB_R2.raw
SB	R3	29	DIA_Data	29_lumos_SB_R3.raw
SC	R1	29	DIA_Data	29_lumos_SC_R1.raw
SC	R2	29	DIA_Data	29_lumos_SC_R2.raw
SC	R3	29	DIA_Data	29_lumos_SC_R3.raw
		29	windows.png	29_windows.png
		29	windows.txt	29_windows.txt
SA	R1	31	DIA_Data	31_lumos_prg_SA_R1.raw
SA	R2	31	DIA_Data	31_lumos_prg_SA_R2.raw
SA	R3	31	DIA_Data	31_lumos_prg_SA_R3.raw
SB	R1	31	DIA_Data	31_lumos_prg_SB_R1.raw
SB	R2	31	DIA_Data	31_lumos_prg_SB_R2.raw
SB	R3	31	DIA_Data	31_lumos_prg_SB_R3.raw
SC	R1	31	DIA_Data	31_lumos_prg_SC_R1.raw
SC	R2	31	DIA_Data	31_lumos_prg_SC_R2.raw
SC	R3	31	DIA_Data	31_lumos_prg_SC_R3.raw
		31	windows.png	31_windows.png
		31	windows.txt	31_windows.txt
		32	CustomLCMethod.csv	32_CustomLCMethod.csv
		32	CustomMSMethod.csv	32_CustomMSMethod.csv
SA	R1	32	DIA_Data	32_lumos_lab_SA_R1.raw
SA	R2	32	DIA_Data	32_lumos_lab_SA_R2.raw
SA	R3	32	DIA_Data	32_lumos_lab_SA_R3.raw
SB	R1	32	DIA_Data	32_lumos_lab_SB_R1.raw
SB	R2	32	DIA_Data	32_lumos_lab_SB_R2.raw
SB	R3	32	DIA_Data	32_lumos_lab_SB_R3.raw
SC	R1	32	DIA_Data	32_lumos_lab_SC_R1.raw
SC	R2	32	DIA_Data	32_lumos_lab_SC_R2.raw
SC	R3	32	DIA_Data	32_lumos_lab_SC_R3.raw

		32	windows.png	32_windows.png
		32	windows.txt	32_windows.txt
SA	R1	33	DIA_Data	33_lumos_prg_SA_R1.raw
SA	R2	33	DIA_Data	33_lumos_prg_SA_R2.raw
SA	R3	33	DIA_Data	33_lumos_prg_SA_R3.raw
SB	R1	33	DIA_Data	33_lumos_prg_SB_R1.raw
SB	R3	33	DIA_Data	33_lumos_prg_SB_R3.raw
SC	R1	33	DIA_Data	33_lumos_prg_SC_R1.raw
SC	R2	33	DIA_Data	33_lumos_prg_SC_R2.raw
SC	R3	33	DIA_Data	33_lumos_prg_SC_R3.raw
		33	windows.png	33_windows.png
		33	windows.txt	33_windows.txt
SA	R1	34	DIA_Data	34_qehf_prg_SA_R1.raw
SA	R2	34	DIA_Data	34_qehf_prg_SA_R2.raw
SA	R3	34	DIA_Data	34_qehf_prg_SA_R3.raw
SB	R1	34	DIA_Data	34_qehf_prg_SB_R1.raw
SB	R2	34	DIA_Data	34_qehf_prg_SB_R2.raw
SB	R3	34	DIA_Data	34_qehf_prg_SB_R3.raw
SC	R1	34	DIA_Data	34_qehf_prg_SC_R1.raw
SC	R2	34	DIA_Data	34_qehf_prg_SC_R2.raw
SC	R3	34	DIA_Data	34_qehf_prg_SC_R3.raw
		34	windows.png	34_windows.png
		34	windows.txt	34_windows.txt
SA	R1	35	DIA_Data	35_qehf_prg_SA_R1.raw
SA	R2	35	DIA_Data	35_qehf_prg_SA_R2.raw
SA	R3	35	DIA_Data	35_qehf_prg_SA_R3.raw
SB	R1	35	DIA_Data	35_qehf_prg_SB_R1.raw
SB	R2	35	DIA_Data	35_qehf_prg_SB_R2.raw
SB	R3	35	DIA_Data	35_qehf_prg_SB_R3.raw
SC	R1	35	DIA_Data	35_qehf_prg_SC_R1.raw
SC	R2	35	DIA_Data	35_qehf_prg_SC_R2.raw
SC	R3	35	DIA_Data	35_qehf_prg_SC_R3.raw
		35	windows.png	35_windows.png
		35	windows.txt	35_windows.txt
		36	CustomLCMethod.csv	36_CustomLCMethod.csv
		36	CustomMSMethod.csv	36_CustomMSMethod.csv
SA	R1	36	DIA_Data	36_qehf_lab_SA_R1.raw
SA	R2	36	DIA_Data	36_qehf_lab_SA_R2.raw
SA	R3	36	DIA_Data	36_qehf_lab_SA_R3.raw
SB	R1	36	DIA_Data	36_qehf_lab_SB_R1.raw
SB	R2	36	DIA_Data	36_qehf_lab_SB_R2.raw
SB	R3	36	DIA_Data	36_qehf_lab_SB_R3.raw
SC	R1	36	DIA_Data	36_qehf_lab_SC_R1.raw
SC	R2	36	DIA_Data	36_qehf_lab_SC_R2.raw
SC	R3	36	DIA_Data	36_qehf_lab_SC_R3.raw
		36	windows.png	36_windows.png

		36	windows.txt	36_windows.txt
SA	R1	37	DIA_Data	37_fusion_prg_SA_R1.raw
SA	R2	37	DIA_Data	37_fusion_prg_SA_R2.raw
SA	R3	37	DIA_Data	37_fusion_prg_SA_R3.raw
SB	R1	37	DIA_Data	37_fusion_prg_SB_R1.raw
SB	R2	37	DIA_Data	37_fusion_prg_SB_R2.raw
SB	R3	37	DIA_Data	37_fusion_prg_SB_R3.raw
SC	R1	37	DIA_Data	37_fusion_prg_SC_R1.raw
SC	R2	37	DIA_Data	37_fusion_prg_SC_R2.raw
SC	R3	37	DIA_Data	37_fusion_prg_SC_R3.raw
		37	windows.png	37_windows.png
		37	windows.txt	37_windows.txt
		39	CustomLCMethod.csv	39_CustomLCMethod.csv
		39	CustomMSMethod.csv	39_CustomMSMethod.csv
SA	R1	39	DIA_Data	39_tt5600_lab_SA_R1.wiff
SA	R1	39	DIA_Data	39_tt5600_lab_SA_R1.wiff.scan
SA	R2	39	DIA_Data	39_tt5600_lab_SA_R2.wiff
SA	R2	39	DIA_Data	39_tt5600_lab_SA_R2.wiff.scan
SA	R3	39	DIA_Data	39_tt5600_lab_SA_R3.wiff
SA	R3	39	DIA_Data	39_tt5600_lab_SA_R3.wiff.scan
SB	R1	39	DIA_Data	39_tt5600_lab_SB_R1.wiff
SB	R1	39	DIA_Data	39_tt5600_lab_SB_R1.wiff.scan
SB	R2	39	DIA_Data	39_tt5600_lab_SB_R2.wiff
SB	R2	39	DIA_Data	39_tt5600_lab_SB_R2.wiff.scan
SB	R3	39	DIA_Data	39_tt5600_lab_SB_R3.wiff
SB	R3	39	DIA_Data	39_tt5600_lab_SB_R3.wiff.scan
SC	R1	39	DIA_Data	39_tt5600_lab_SC_R1.wiff
SC	R1	39	DIA_Data	39_tt5600_lab_SC_R1.wiff.scan
SC	R2	39	DIA_Data	39_tt5600_lab_SC_R2.wiff
SC	R2	39	DIA_Data	39_tt5600_lab_SC_R2.wiff.scan
SC	R3	39	DIA_Data	39_tt5600_lab_SC_R3.wiff
SC	R3	39	DIA_Data	39_tt5600_lab_SC_R3.wiff.scan
		39	windows.png	39_windows.png
		39	windows.txt	39_windows.txt
SA	R1	44	DIA_Data	44_qehfx_prg_SA_R1.raw
SA	R2	44	DIA_Data	44_qehfx_prg_SA_R2.raw
SA	R3	44	DIA_Data	44_qehfx_prg_SA_R3.raw
SB	R1	44	DIA_Data	44_qehfx_prg_SB_R1.raw
SB	R2	44	DIA_Data	44_qehfx_prg_SB_R2.raw
SB	R3	44	DIA_Data	44_qehfx_prg_SB_R3.raw
SC	R1	44	DIA_Data	44_qehfx_prg_SC_R1.raw
SC	R2	44	DIA_Data	44_qehfx_prg_SC_R2.raw
SC	R3	44	DIA_Data	44_qehfx_prg_SC_R3.raw
		44	windows.png	44_windows.png
		44	windows.txt	44_windows.txt
SA	R1	45	DIA_Data	45_qeplus_prg_SA_R1.raw

SA	R2	45	DIA_Data	45_qeplus_prg_SA_R2.raw
SA	R3	45	DIA_Data	45_qeplus_prg_SA_R3.raw
SB	R1	45	DIA_Data	45_qeplus_prg_SB_R1.raw
SB	R2	45	DIA_Data	45_qeplus_prg_SB_R2.raw
SB	R3	45	DIA_Data	45_qeplus_prg_SB_R3.raw
SC	R1	45	DIA_Data	45_qeplus_prg_SC_R1.raw
SC	R2	45	DIA_Data	45_qeplus_prg_SC_R2.raw
SC	R3	45	DIA_Data	45_qeplus_prg_SC_R3.raw
		45	windows.png	45_windows.png
		45	windows.txt	45_windows.txt
		46	CustomLCMethod.csv	46_CustomLCMethod.csv
		46	CustomMSMethod.csv	46_CustomMSMethod.csv
		46	windows.png	46_lab_method_windows.png
		46	windows.txt	46_lab_method_windows.txt
SA	R1	46	DIA_Data	46_lumos_lab_SA_R1.raw
SA	R2	46	DIA_Data	46_lumos_lab_SA_R2.raw
SA	R3	46	DIA_Data	46_lumos_lab_SA_R3.raw
SB	R1	46	DIA_Data	46_lumos_lab_SB_R1.raw
SB	R2	46	DIA_Data	46_lumos_lab_SB_R2.raw
SB	R3	46	DIA_Data	46_lumos_lab_SB_R3.raw
SC	R1	46	DIA_Data	46_lumos_lab_SC_R1.raw
SC	R2	46	DIA_Data	46_lumos_lab_SC_R2.raw
SC	R3	46	DIA_Data	46_lumos_lab_SC_R3.raw
SA	R1	46	DIA_Data	46_lumos_prg_SA_R1.raw
SA	R2	46	DIA_Data	46_lumos_prg_SA_R2.raw
SA	R3	46	DIA_Data	46_lumos_prg_SA_R3.raw
SA	R4	46	DIA_Data	46_lumos_prg_SA_R4.raw
SB	R1	46	DIA_Data	46_lumos_prg_SB_R1.raw
SB	R2	46	DIA_Data	46_lumos_prg_SB_R2.raw
SB	R3	46	DIA_Data	46_lumos_prg_SB_R3.raw
SB	R4	46	DIA_Data	46_lumos_prg_SB_R4.raw
SC	R1	46	DIA_Data	46_lumos_prg_SC_R1.raw
SC	R2	46	DIA_Data	46_lumos_prg_SC_R2.raw
SC	R3	46	DIA_Data	46_lumos_prg_SC_R3.raw
SC	R4	46	DIA_Data	46_lumos_prg_SC_R4.raw
		46	windows.png	46_prg_method_windows.png
		46	windows.txt	46_prg_method_windows.txt
		47	CustomLCMethod.csv	47_CustomLCMethod.csv
		47	CustomMSMethod.csv	47_CustomMSMethod.csv
		47	instrument_method	47_DIA_PRG_25wind_24mz_400_1000.meth
SA	R1	47	DIA_Data	47_qe_lab_SA_R1.raw
SA	R2	47	DIA_Data	47_qe_lab_SA_R2.raw
SA	R3	47	DIA_Data	47_qe_lab_SA_R3.raw
SB	R1	47	DIA_Data	47_qe_lab_SB_R1.raw
SB	R2	47	DIA_Data	47_qe_lab_SB_R2.raw
SB	R3	47	DIA_Data	47_qe_lab_SB_R3.raw

SC	R1	47	DIA_Data	47_qe_lab_SC_R1.raw
SC	R2	47	DIA_Data	47_qe_lab_SC_R2.raw
SC	R3	47	DIA_Data	47_qe_lab_SC_R3.raw
		47	windows.png	47_windows.png
		47	windows.txt	47_windows.txt
SA	R1	48	DIA_Data	48_lumos_prg_SA_R1.raw
SA	R2	48	DIA_Data	48_lumos_prg_SA_R2.raw
SA	R3	48	DIA_Data	48_lumos_prg_SA_R3.raw
SB	R1	48	DIA_Data	48_lumos_prg_SB_R1.raw
SB	R2	48	DIA_Data	48_lumos_prg_SB_R2.raw
SB	R3	48	DIA_Data	48_lumos_prg_SB_R3.raw
SC	R1	48	DIA_Data	48_lumos_prg_SC_R1.raw
SC	R2	48	DIA_Data	48_lumos_prg_SC_R2.raw
SC	R3	48	DIA_Data	48_lumos_prg_SC_R3.raw
SA	R1	48	DIA_Data	48_qehfx_prg_SA_R1.raw
SA	R2	48	DIA_Data	48_qehfx_prg_SA_R2.raw
SA	R3	48	DIA_Data	48_qehfx_prg_SA_R3.raw
SB	R1	48	DIA_Data	48_qehfx_prg_SB_R1.raw
SB	R2	48	DIA_Data	48_qehfx_prg_SB_R2.raw
SB	R3	48	DIA_Data	48_qehfx_prg_SB_R3.raw
SC	R1	48	DIA_Data	48_qehfx_prg_SC_R1.raw
SC	R2	48	DIA_Data	48_qehfx_prg_SC_R2.raw
SC	R3	48	DIA_Data	48_qehfx_prg_SC_R3.raw
		48	windows-lumos.png	48_windows-lumos.png
		48	windows-lumos.txt	48_windows-lumos.txt
		48	windows-qehfx.png	48_windows-qehfx.png
		48	windows-qehfx.txt	48_windows-qehfx.txt
		49	CustomMSMethod.csv	49_CustomMSMethod.csv
		49	CustomIsolationWindows.csv	49_CustomIsolationWindows.csv
SA	R1	49	DIA_Data	49_qe_lab_SA_R1.raw
SA	R2	49	DIA_Data	49_qe_lab_SA_R2.raw
SA	R3	49	DIA_Data	49_qe_lab_SA_R3.raw
SB	R1	49	DIA_Data	49_qe_lab_SB_R1.raw
SB	R2	49	DIA_Data	49_qe_lab_SB_R2.raw
SB	R3	49	DIA_Data	49_qe_lab_SB_R3.raw
SC	R1	49	DIA_Data	49_qe_lab_SC_R1.raw
SC	R2	49	DIA_Data	49_qe_lab_SC_R2.raw
SC	R3	49	DIA_Data	49_qe_lab_SC_R3.raw
		49	windows.png	49_windows.png
		49	windows.txt	49_windows.txt
		50	CustomLCMethod.csv	50_CustomLCMethod.csv
SA	R1	50	DIA_Data	50_qehfx_prg_SA_R1.raw
SA	R2	50	DIA_Data	50_qehfx_prg_SA_R2.raw
SA	R3	50	DIA_Data	50_qehfx_prg_SA_R3.raw
SB	R1	50	DIA_Data	50_qehfx_prg_SB_R1.raw
SB	R2	50	DIA_Data	50_qehfx_prg_SB_R2.raw

SB	R3	50	DIA_Data	50_qehfx_prg_SB_R3.raw
SC	R1	50	DIA_Data	50_qehfx_prg_SC_R1.raw
SC	R2	50	DIA_Data	50_qehfx_prg_SC_R2.raw
SC	R3	50	DIA_Data	50_qehfx_prg_SC_R3.raw
		50	windows.png	50_windows.png
		50	windows.txt	50_windows.txt
SA	R1	52	DIA_Data	52_fusion_lab_SA_R1.raw
SA	R2	52	DIA_Data	52_fusion_lab_SA_R2.raw
SA	R3	52	DIA_Data	52_fusion_lab_SA_R3.raw
SB	R1	52	DIA_Data	52_fusion_lab_SB_R1.raw
SB	R2	52	DIA_Data	52_fusion_lab_SB_R2.raw
SB	R3	52	DIA_Data	52_fusion_lab_SB_R3.raw
SC	R1	52	DIA_Data	52_fusion_lab_SC_R1.raw
SC	R2	52	DIA_Data	52_fusion_lab_SC_R2.raw
SC	R3	52	DIA_Data	52_fusion_lab_SC_R3.raw
		52	windows.png	52_windows.png
		52	windows.txt	52_windows.txt
SA	R1	53	DIA_Data	53_qe_prg_SA_R1.raw
SA	R2	53	DIA_Data	53_qe_prg_SA_R2.raw
SA	R3	53	DIA_Data	53_qe_prg_SA_R3.raw
SB	R1	53	DIA_Data	53_qe_prg_SB_R1.raw
SB	R2	53	DIA_Data	53_qe_prg_SB_R2.raw
SB	R3	53	DIA_Data	53_qe_prg_SB_R3.raw
SC	R1	53	DIA_Data	53_qe_prg_SC_R1.raw
SC	R2	53	DIA_Data	53_qe_prg_SC_R2.raw
SC	R3	53	DIA_Data	53_qe_prg_SC_R3.raw
		53	windows.png	53_windows.png
		53	windows.txt	53_windows.txt
		54	CustomLCMethod.csv	54_CustomLCMethod_bandh.csv
		54	CustomMSMethod.csv	54_CustomMSMethod_b.csv
		54	CustomMSMethod.csv	54_CustomMSMethod_h.csv
		54	instrument_method	54_DIA_140min_b.meth
		54	instrument_method	54_DIA_140min_h.meth
SA	R1	54	DIA_Data	54_qeplus_lab_b_SA_R1.raw
SA	R2	54	DIA_Data	54_qeplus_lab_b_SA_R2.raw
SA	R3	54	DIA_Data	54_qeplus_lab_b_SA_R3.raw
SB	R1	54	DIA_Data	54_qeplus_lab_b_SB_R1.raw
SB	R2	54	DIA_Data	54_qeplus_lab_b_SB_R2.raw
SB	R3	54	DIA_Data	54_qeplus_lab_b_SB_R3.raw
SC	R1	54	DIA_Data	54_qeplus_lab_b_SC_R1.raw
SC	R2	54	DIA_Data	54_qeplus_lab_b_SC_R2.raw
SC	R3	54	DIA_Data	54_qeplus_lab_b_SC_R3.raw
SA	R1	54	DIA_Data	54_qeplus_lab_h_SA_R1.raw
SA	R2	54	DIA_Data	54_qeplus_lab_h_SA_R2.raw
SA	R3	54	DIA_Data	54_qeplus_lab_h_SA_R3.raw
SB	R1	54	DIA_Data	54_qeplus_lab_h_SB_R1.raw

SB	R2	54	DIA_Data	54_qeplus_lab_h_SB_R2.raw
SB	R3	54	DIA_Data	54_qeplus_lab_h_SB_R3.raw
SC	R1	54	DIA_Data	54_qeplus_lab_h_SC_R1.raw
SC	R2	54	DIA_Data	54_qeplus_lab_h_SC_R2.raw
SC	R3	54	DIA_Data	54_qeplus_lab_h_SC_R3.raw
		54	windows.png	54_windows-b.png
		54	windows.txt	54_windows-b.txt
		54	windows.png	54_windows-h.png
		54	windows.txt	54_windows-h.txt
		55	CustomLCMethod.csv	55_CustomLCMethod.csv
		55	CustomMSMethod.csv	55_CustomMSMethod.csv
SA	R1	55	DIA_Data	55_qehf_lab_SA_R1.raw
SB	R1	55	DIA_Data	55_qehf_lab_SB_R1.raw
SC	R1	55	DIA_Data	55_qehf_lab_SC_R1.raw
		55	windows.png	55_windows.png
		55	windows.txt	55_windows.txt
		56	CustomMSMethod.csv	56_CustomMSMethod.csv
SA	R1	56	DIA_Data	56_orbivep_lab_SA_R1.raw
SA	R2	56	DIA_Data	56_orbivep_lab_SA_R2.raw
SA	R3	56	DIA_Data	56_orbivep_lab_SA_R3.raw
SB	R1	56	DIA_Data	56_orbivep_lab_SB_R1.raw
SB	R2	56	DIA_Data	56_orbivep_lab_SB_R2.raw
SB	R3	56	DIA_Data	56_orbivep_lab_SB_R3.raw
SC	R1	56	DIA_Data	56_orbivep_lab_SC_R1.raw
SC	R2	56	DIA_Data	56_orbivep_lab_SC_R2.raw
SC	R3	56	DIA_Data	56_orbivep_lab_SC_R3.raw
		56	windows.png	56_windows.png
		56	windows.txt	56_windows.txt
SA	R1	57	DIA_Data	57_qehfx_prg_SA_R1.raw
SA	R2	57	DIA_Data	57_qehfx_prg_SA_R2.raw
SA	R3	57	DIA_Data	57_qehfx_prg_SA_R3.raw
SB	R1	57	DIA_Data	57_qehfx_prg_SB_R1.raw
SB	R2	57	DIA_Data	57_qehfx_prg_SB_R2.raw
SB	R3	57	DIA_Data	57_qehfx_prg_SB_R3.raw
SC	R1	57	DIA_Data	57_qehfx_prg_SC_R1.raw
SC	R2	57	DIA_Data	57_qehfx_prg_SC_R2.raw
SC	R3	57	DIA_Data	57_qehfx_prg_SC_R3.raw
		57	windows.png	57_windows.png
		57	windows.txt	57_windows.txt
		60	CustomLCMethod.csv	60_CustomLCMethod.csv
SA	R1	60	DIA_Data	60_lumos_lab_SA_R1.raw
SA	R2	60	DIA_Data	60_lumos_lab_SA_R2.raw
SA	R3	60	DIA_Data	60_lumos_lab_SA_R3.raw
SB	R1	60	DIA_Data	60_lumos_lab_SB_R1.raw
SB	R2	60	DIA_Data	60_lumos_lab_SB_R2.raw
SB	R3	60	DIA_Data	60_lumos_lab_SB_R3.raw

SC	R1	60	DIA_Data	60_lumos_lab_SC_R1.raw
SC	R2	60	DIA_Data	60_lumos_lab_SC_R2.raw
SC	R3	60	DIA_Data	60_lumos_lab_SC_R3.raw
		60	windows.png	60_windows.png
		60	windows.txt	60_windows.txt
		63	CustomLCMethod.csv	63_CustomLCMethod.csv
		63	CustomMSMethod.csv	63_CustomMSMethod.csv
SA	R1	63	DIA_Data	63_lumos_prg_SA_R1.raw
SA	R2	63	DIA_Data	63_lumos_prg_SA_R2.raw
SA	R3	63	DIA_Data	63_lumos_prg_SA_R3.raw
SB	R1	63	DIA_Data	63_lumos_prg_SB_R1.raw
SB	R2	63	DIA_Data	63_lumos_prg_SB_R2.raw
SB	R3	63	DIA_Data	63_lumos_prg_SB_R3.raw
SC	R1	63	DIA_Data	63_lumos_prg_SC_R1.raw
SC	R2	63	DIA_Data	63_lumos_prg_SC_R2.raw
SC	R3	63	DIA_Data	63_lumos_prg_SC_R3.raw
		63	windows.png	63_windows.png
		63	windows.txt	63_windows.txt
Pool	R1	03	DDA_Data	03_lumos_prg_DDA_pool_R1.raw
Pool	R2	03	DDA_Data	03_lumos_prg_DDA_pool_R2.raw
Pool	R3	03	DDA_Data	03_lumos_prg_DDA_pool_R3.raw
Pool		03	GPF_Data	03_lumos_prg_DIA_GPF1.raw
Pool		03	GPF_Data	03_lumos_prg_DIA_GPF2.raw
Pool		03	GPF_Data	03_lumos_prg_DIA_GPF3.raw
Pool		03	GPF_Data	03_lumos_prg_DIA_GPF4.raw
Pool		03	GPF_Data	03_lumos_prg_DIA_GPF5.raw
Pool	R1	48	DDA_Data	48_lumos_prg_DDA_pool_R1.raw
Pool	R2	48	DDA_Data	48_lumos_prg_DDA_pool_R2.raw
Pool	R3	48	DDA_Data	48_lumos_prg_DDA_pool_R3.raw
Spikes		48	DDA_Data	48_qehfx_PRGspikes_100fmol_DDA.raw
Spikes		48	DIA_Data	48_qehfx_PRGspikes_100fmol_DIA.raw
Spikes		48	DDA_Data	48_qehfx_PRGspikes_200fmol_DDA.raw
Spikes		48	DIA_Data	48_qehfx_PRGspikes_200fmol_DIA.raw
Spikes		48	DDA_Data	48_qehfx_PRGspikes_500fmol_DDA.raw
Spikes		48	DIA_Data	48_qehfx_PRGspikes_500fmol_DIA.raw
Spikes		48	DIA_Data	48_qehfx_PRGspikes_800fmol_DIA.raw
Spikes		48	DDA_Data	48_qehfx_PRGspikess_800fmol_DDA.raw
Pool	R1	48	DDA_Data	48_qehfx_prg_DDA_pool_R1.raw
Pool	R2	48	DDA_Data	48_qehfx_prg_DDA_pool_R2.raw
Pool	R3	48	DDA_Data	48_qehfx_prg_DDA_pool_R3.raw
			EncyclopeDIA Spectral Library	combined_prg_pan_human.dlib
			EncyclopeDIA Spectral Library	combined_prg_sprothuman.dlib
			FASTA	contaminants_20120713.fasta
			FASTA	sp_human_180620_plus_PRG_ABRF_4_prot.fasta
			Scaffold Chromatogram Library	03 - PH plus CL library.elib

Scaffold Chromatogram Library	03 - Prosit plus CL library.elib
Scaffold Chromatogram Library	03 Chromatogram Library.elib
Scaffold Experiment	03 - CL only.sdia
Scaffold Experiment	03 - PH plus CL.sdia
Scaffold Experiment	03 - Prosit plus CL.sdia
Scaffold Results Export	03 - CL only - ABRF Spike Proteins.csv
Scaffold Results Export	03 - PH plus CL - ABRF Spike Proteins.csv
Scaffold Results Export	03 - Prosit plus CL - ABRF Spike Proteins.csv
Scaffold Results Export	Peptide Match Report of 03 - CL only.csv
Scaffold Results Export	Peptide Match Report of 03 - PH plus CL.csv
Scaffold Results Export	Peptide Match Report of 03 - Prosit plus CL.csv
Scaffold Results Export	Samples Report of 03 - CL only.csv
Scaffold Results Export	Samples Report of 03 - PH plus CL.csv
Scaffold Results Export	Samples Report of 03 - Prosit plus CL.csv
Scaffold Results Export	Samples Table of 03 - CL only.csv
Scaffold Results Export	Samples Table of 03 - PH plus CL.csv
Scaffold Results Export	Samples Table of 03 - Prosit plus CL.csv
Spectronaut Experiment	03_48_against_combined_DpD.sne
Spectronaut Experiment	03_48_Pan_human_Spike_lib.sne
Spectronaut Experiment	03_against_48_DpD.sne
Spectronaut Experiment	03_lumos_directDIA.sne
Spectronaut Experiment	03_Lumos_own_DpD.sne
Spectronaut Experiment	48_against_03_DpD.sne
Spectronaut Experiment	48_lumos_directDIA.sne
Spectronaut Experiment	48_lumos_own_DpD.sne
Spectronaut Export	03_48_against_combined_DpD_new_ExperimentAnalysis.txt
Spectronaut Export	03_48_against_combined_DpD_new_IdentificationsOverview.tsv
Spectronaut Export	03_48_against_combined_DpD_new_PGReport.xlsx
Spectronaut Export	03_48_Pan_human_Spike_lib_ExperimentAnalysis.txt
Spectronaut Export	03_48_Pan_human_Spike_lib_IdentificationsOverview.tsv
Spectronaut Export	03_48_Pan_human_Spike_lib_PGReport.xlsx
Spectronaut Export	03_against_48_DpD_new_SA_lib_ExperimentAnalysis.txt
Spectronaut Export	03_against_48_DpD_new_SA_lib_IdentificationsOverview.tsv
Spectronaut Export	03_against_48_DpD_new_SA_lib_PGReport.xlsx
Spectronaut Export	03_lumos_directDIA_ExperimentAnalysis.txt
Spectronaut Export	03_lumos_directDIA_IdentificationsOverview.tsv
Spectronaut Export	03_lumos_directDIA_PGReport.xlsx
Spectronaut Export	03_Lumos_own_DpD_ExperimentAnalysis.txt
Spectronaut Export	03_Lumos_own_DpD_IdentificationsOverview.tsv
Spectronaut Export	03_Lumos_own_DpD_PGReport.xlsx
Spectronaut Export	48_Lumos_against_DpD_03_lib_ExperimentAnalysis.txt
Spectronaut Export	48_Lumos_against_DpD_03_lib_IdentificationsOverview.tsv
Spectronaut Export	48_Lumos_against_DpD_03_lib_PGReport.xlsx
Spectronaut Export	48_lumos_directDIA_ExperimentAnalysis.txt
Spectronaut Export	48_lumos_directDIA_IdentificationsOverview.tsv

Spectronaut Export	48_lumos_directDIA_PGReport.xlsx
Spectronaut Export	48_lumos_own_DpD_new_ExperimentAnalysis.txt
Spectronaut Export	48_lumos_own_DpD_new_IdentificationsOverview.tsv
Spectronaut Export	48_lumos_own_DpD_new_PGReport.xlsx
Spectronaut Spectral Library	03_lumos_48_lumos_DpD.kit
Spectronaut Spectral Library	03_lumos_48_lumos_DpD.xls
Spectronaut Spectral Library	03_lumos_directDIA.kit
Spectronaut Spectral Library	03_lumos_directDIA.xls
Spectronaut Spectral Library	03_lumos_DpD.kit
Spectronaut Spectral Library	03_lumos_DpD.xls
Spectronaut Spectral Library	48_lumos_directDIA.kit
Spectronaut Spectral Library	48_lumos_directDIA.xls
Spectronaut Spectral Library	48_lumos_DpD.kit
Spectronaut Spectral Library	48_lumos_DpD.xls
Spectronaut Spectral Library	48_qehfx_spikes_DpD.kit
Spectronaut Spectral Library	48_qehfx_spikes_DpD.xls
Spectronaut Spectral Library	Pan Human Library - ETH.kit
Spectronaut Spectral Library	Pan Human Library - ETH.xls
Metadata for 49 Data Sets	Online-only Table 1.xlsx

.

Technical Validation

Data return and curation

Participants uploaded their data to a private FTP hosted by MassIVE. Each participant was given a folder designated by their participant number and the file naming scheme was described in Supplemental File 1. The instrument naming scheme was changed for Online-only Table 1 to reflect instrument names, following the PSI-MS recommended names (https://github.com/HUPO-PSI/psi-ms-CV/blob/master/psi-ms.obo). Following the end of the study, file integrity was confirmed by opening each file. In some cases, the file was corrupt and the participant requested by the anonymiser to re-uploaded the files. In some cases, the original file was also corrupt and those data were not available. In the case of missing files, we made every effort with the participant to find and upload the missing data. Despite these efforts, not all participants were able to provide the requested nine raw data files.

Once the data was curated, files were manually inspected using the TIC to look for any noticeable qualities such as TIC without peaks. Notes were made in Online-only Table 1. The majority of replicates were consistent, though it should be noted that this does not imply a measure of data quality. Next, the embedded parameters in the raw files were used to determine and or confirm MS-acquisition settings. Though participants were encouraged to self-report MS settings, there was missing information and discrepancies. To avoid reliance on the participant, the first replicate of sample A was used to determine DIA window scheme, MS1 and MS2 resolution (and injection time if applicable) and DIA cycle time. All other files from that participant were assumed to have the same acquisition settings. In the case of Sciex TripleTOFs, participants reported MS1 and MS2 settings. The DIA windowing strategy was determined using Skyline[34], while the scan header provided MS1 and MS2 information (in the case of Thermo instruments). The DIA cycle time was determined using Spectronaut (v13.6.190905.43655; Biognosys AG)[28]. This information is provided in Online-only Table 1.

Although LC conditions were not available from data files many participants submitted LC gradient specifics along with raw data. These are included as “supplemental” in Online-only Table 1, and are available in the MassIVE MSV000086479. Finally, in case where those metadata couldn’t be surmised and were not self-reported, we contacted the participant directly to request that information. After these efforts, there are still some participants with missing information. This is noted in Online-only Table 1.

Survey

Participants were given the option to self-report the specific LC columns they used. the HPLC parameters, the MS instrument settings and any attempt to identify the amount of spike in proteins in the labelled samples. These survey questions are provided in Supplemental File 2.

Usage Notes

All raw files are available on MassIVE MSV000086479, and many programs can use these files directly. Software to analyse DIA includes, but is not limited to: DIA-NN[35], DIA-Umpire[36], EncyclopeDIA[25], OpenSWATH[37], PEAKS Studio X (Bioinformatics Solutions, Inc.), PECAN[38], Protalizer (Vulcan Analytical), Scaffold DIA (Proteome Software), Skyline[34], and Spectronaut (Biognosys AG)[28] as well as DIA specific statistical packages (ex. iq: Protein Quantification in Mass Spectrometry-Based Proteomics; https://CRAN.R-project.org/package=iq). Many of these programs have excellent online resources including tutorials of the analysis pipeline. The relevant information such as DIA window placement or instrument settings can be found in Online-only Table 1 and in supplemental files on MassIVE MSV000086479. Specifically to the analysis performed in this paper, we have included .sne (Spectronaut) and .sdia (Scaffold DIA) files, which are located on MassIVE MSV000086479 and can be

opened with free viewers for these programs. The libraries used in the analysis can be found on MassIVE MSV000086479 as .kit, .xls, .dlib or .elib files and can be used directly by some of the software listed. Alternatively, the DDA files available on MassIVE MSV000086479 can be used to create libraries. It should be noted that all samples included the iRT peptides which can be used, if needed, to map the elution patterns into iRT space. Finally, in the case of *in silico* libraries such as Prosit[19] and MS2PIP[21,23], the original publication or tutorials should be consulted for instructions for how to combine with empirical data[20].

Code Availability

Analysis of raw data performed using Spectronaut (v13.6.190905.43655; Biognosys AG)[28] and Scaffold DIA (v1.3.1; Proteome Software). No other code was used for this data generation or example analysis.

Author contributions

BN assisted in study design and execution, analysed data, curated study data, wrote manuscript with contributions from all authors.

PS assisted in study design and execution, prepared experimental samples, feedback and edits on manuscript.

BCS assisted with data analysis, design and generation of figures, feedback and edits on manuscript.

LH assisted in study design and execution, design and generation of figures, feedback and edits on manuscript

LM assisted in study design and execution, feedback and edits on manuscript.

MM assisted in study design and execution, feedback and edits on manuscript.

BP assisted in study design and execution, feedback and edits on manuscript.

BS assisted in study design and execution, feedback and edits on manuscript.

MP assisted in study design and execution, feedback and edits on manuscript.

YW assisted in study design and execution, developed participant survey, feedback and edits on manuscript.

PJ assisted in study design and execution, feedback and edits on manuscript.

JK assisted in study design and execution, analysed data, wrote manuscript with contributions from all authors.

Acknowledgements

The authors wish to thank Matt Herring for graphical advice when designing figures. Identification of certain commercial equipment, instruments, software or materials does not imply recommendation or endorsement by the National Institute of Standards and Technology, nor does it imply that the products identified are necessarily the best available for the purpose. P.D.J was supported by National Cancer Institute - Informatics Technology for Cancer Research (NCI-ITCR) grant 1U24CA199347 and National Science Foundation (U.S.) grant 1458524. We would also like to thank the software companies (Biognosys AG, Bioinformatics Solutions, Inc., and Proteome Software for providing extended trial licences of their software to study participants and Biognosys AG for the provision of the iRT peptides added to all samples.

Competing interests

B.C.S. is a founder and shareholder in Proteome Software, which operates in the field of proteomics. B.S. is the CEO at Bioinformatics Solutions Inc., which creates software for the field of proteomics. The other authors declare no competing interests.

References

1 Hu, A., Noble, W. S. & Wolf-Yadlin, A. Technical advances in proteomics: new developments in data-independent acquisition. *F1000Research* **5**, doi:10.12688/f1000research.7042.1 (2016).

2 Ting, Y. S. *et al.* Peptide-Centric Proteome Analysis: An Alternative Strategy for the Analysis of Tandem Mass Spectrometry Data. *Molecular & cellular proteomics : MCP* **14**, 2301-2307, doi:10.1074/mcp.O114.047035 (2015).

3 Bilbao, A. *et al.* Processing strategies and software solutions for data-independent acquisition in mass spectrometry. *Proteomics* **15**, 964-980, doi:10.1002/pmic.201400323 (2015).

4 Reubsaet, L., Sweredoski, M. J. & Moradian, A. Data-Independent Acquisition for the Orbitrap Q Exactive HF: A Tutorial. *Journal of proteome research* **18**, 803-813, doi:10.1021/acs.jproteome.8b00845 (2019).

5 Muntel, J. *et al.* Surpassing 10 000 identified and quantified proteins in a single run by optimizing current LC-MS instrumentation and data analysis strategy. *Molecular omics*, doi:10.1039/c9mo00082h (2019).

6 Bache, N. *et al.* A Novel LC System Embeds Analytes in Pre-formed Gradients for Rapid, Ultra-robust Proteomics. *Molecular & cellular proteomics : MCP* **17**, 2284-2296, doi:10.1074/mcp.TIR118.000853 (2018).

7 Ludwig, C. *et al.* Data-independent acquisition-based SWATH-MS for quantitative proteomics: a tutorial. *Molecular systems biology* **14**, e8126, doi:10.15252/msb.20178126 (2018).

8 Bruderer, R. *et al.* Optimization of Experimental Parameters in Data-Independent Mass Spectrometry Significantly Increases Depth and Reproducibility of Results. *Molecular & cellular proteomics : MCP* **16**, 2296-2309, doi:10.1074/mcp.RA117.000314 (2017).

9 Pino, L. K., Just, S. C., MacCoss, M. J. & Searle, B. C. Acquiring and Analyzing Data Independent Acquisition Proteomics Experiments without Spectrum Libraries. *Molecular & cellular proteomics : MCP* **19**, 1088-1103, doi:10.1074/mcp.P119.001913 (2020).

10 Navarro, P. *et al.* A multicenter study benchmarks software tools for label-free proteome quantification. *Nature biotechnology* **34**, 1130-1136, doi:10.1038/nbt.3685 (2016).

11 Cox, J. *et al.* Accurate proteome-wide label-free quantification by delayed normalization and maximal peptide ratio extraction, termed MaxLFQ. *Molecular & cellular proteomics : MCP* **13**, 2513-2526, doi:10.1074/mcp.M113.031591 (2014).

12 van Riper, S. *et al.* Identification of Low Abundance Proteins in a Highly Complex Protein Mixture. *Zenodo*, doi:10.5281/zenodo.3563207 (2015).

13 Pino, L. K. *et al.* Calibration Using a Single-Point External Reference Material Harmonizes Quantitative Mass Spectrometry Proteomics Data between Platforms and Laboratories. *Analytical chemistry* **90**, 13112-13117, doi:10.1021/acs.analchem.8b04581 (2018).

14 Searle, B. C., Egertson, J. D., Bollinger, J. G., Stergachis, A. B. & MacCoss, M. J. Using Data Independent Acquisition (DIA) to Model High-responding Peptides for Targeted Proteomics Experiments. *Molecular & cellular proteomics : MCP* **14**, 2331-2340, doi:10.1074/mcp.M115.051300 (2015).

15 ABRF. *Proteomics Research Group (PRG)*, <https://abrf.org/research-group/proteomics-research-group-prg> (2018).

16 Collins, B. C. *et al.* Multi-laboratory assessment of reproducibility, qualitative and quantitative performance of SWATH-mass spectrometry. *Nature communications* **8**, 291, doi:10.1038/s41467-017-00249-5 (2017).

17 Barkovits, K. *et al.* Reproducibility, specificity and accuracy of relative quantification using spectral library-based data-independent acquisition. *Molecular & cellular proteomics : MCP*, doi:10.1074/mcp.RA119.001714 (2019).

18 Huang, T. *et al.* Combining Precursor and Fragment Information for Improved Detection of Differential Abundance in Data Independent Acquisition. *Molecular & cellular proteomics : MCP* **19**, 421-430, doi:10.1074/mcp.RA119.001705 (2020).

19 Gessulat, S. *et al.* Prosit: proteome-wide prediction of peptide tandem mass spectra by deep learning. *Nature methods* **16**, 509-518, doi:10.1038/s41592-019-0426-7 (2019).

20 Searle, B. C. *et al.* Generating high-quality libraries for DIA-MS with empirically-corrected peptide predictions. *bioRxiv*, 682245, doi:10.1101/682245 (2019).

21 Gabriels, R., Martens, L. & Degroeve, S. Updated MS(2)PIP web server delivers fast and accurate MS(2) peak intensity prediction for multiple fragmentation methods, instruments and labeling techniques. *Nucleic acids research* **47**, W295-w299, doi:10.1093/nar/gkz299 (2019).

22 Liu, K., Li, S., Wang, L., Ye, Y. & Tang, H. Full-Spectrum Prediction of Peptides Tandem Mass Spectra using Deep Neural Network. *Analytical chemistry* **92**, 4275-4283, doi:10.1021/acs.analchem.9b04867 (2020).

23 Van Puyvelde, B. *et al.* Removing the Hidden Data Dependency of DIA with Predicted Spectral Libraries. *Proteomics* **20**, e1900306, doi:10.1002/pmic.201900306 (2020).

24 Gill, S. C. & von Hippel, P. H. Calculation of protein extinction coefficients from amino acid sequence data. *Analytical biochemistry* **182**, 319-326, doi:10.1016/0003-2697(89)90602-7 (1989).

25 Searle, B. C. *et al.* Chromatogram libraries improve peptide detection and quantification by data independent acquisition mass spectrometry. *Nature communications* **9**, 5128, doi:10.1038/s41467-018-07454-w (2018).

26 Rosenberger, G. *et al.* A repository of assays to quantify 10,000 human proteins by SWATH-MS. *Scientific data* **1**, 140031, doi:10.1038/sdata.2014.31 (2014).

27 Wang, Y. *et al.* ABRF PRG study to evaluate data-independent acquisition for protein quantification in core facility settings. *Zenodo*, doi:10.5281/zenodo.3946819.

28 Bruderer, R. *et al.* Extending the limits of quantitative proteome profiling with data-independent acquisition and application to acetaminophen-treated three-dimensional liver microtissues. *Molecular & cellular proteomics : MCP* **14**, 1400-1410, doi:10.1074/mcp.M114.044305 (2015).

29 Chambers, M. C. *et al.* A cross-platform toolkit for mass spectrometry and proteomics. *Nature biotechnology* **30**, 918-920, doi:10.1038/nbt.2377 (2012).

30 Kall, L., Canterbury, J. D., Weston, J., Noble, W. S. & MacCoss, M. J. Semi-supervised learning for peptide identification from shotgun proteomics datasets. *Nature methods* **4**, 923-925, doi:10.1038/nmeth1113 (2007).

31 Kall, L., Storey, J. D., MacCoss, M. J. & Noble, W. S. Assigning significance to peptides identified by tandem mass spectrometry using decoy databases. *Journal of proteome research* **7**, 29-34, doi:10.1021/pr700600n (2008).

32 Kall, L., Storey, J. D. & Noble, W. S. Non-parametric estimation of posterior error probabilities associated with peptides identified by tandem mass spectrometry. *Bioinformatics (Oxford, England)* **24**, i42-48, doi:10.1093/bioinformatics/btn294 (2008).

33 Ritchie, M. E. *et al.* limma powers differential expression analyses for RNA-sequencing and microarray studies. *Nucleic acids research* **43**, e47, doi:10.1093/nar/gkv007 (2015).

34 MacLean, B. *et al.* Skyline: an open source document editor for creating and analyzing targeted proteomics experiments. *Bioinformatics (Oxford, England)* **26**, 966-968, doi:10.1093/bioinformatics/btq054 (2010).

35 Demichev, V., Messner, C. B., Vernardis, S. I., Lilley, K. S. & Ralser, M. DIA-NN: Neural networks and interference correction enable deep coverage in high-throughput proteomics. *bioRxiv*, 282699, doi:10.1101/282699 (2018).

36 Tsou, C. C. *et al.* DIA-Umpire: comprehensive computational framework for data-independent acquisition proteomics. *Nature methods* **12**, 258-264, 257 p following 264, doi:10.1038/nmeth.3255 (2015).

37 Rost, H. L., Aebersold, R. & Schubert, O. T. Automated SWATH Data Analysis Using Targeted Extraction of Ion Chromatograms. *Methods in molecular biology (Clifton, N.J.)* **1550**, 289-307, doi:10.1007/978-1-4939-6747-6_20 (2017).

38 Ting, Y. S. *et al.* PECAN: library-free peptide detection for data-independent acquisition tandem mass spectrometry data. *Nature methods* **14**, 903-908, doi:10.1038/nmeth.4390 (2017).